Consequences of Strain in $(CH)_8$ Hydrocarbons[1]

KARIN HASSENRÜCK and HANS-DIETER MARTIN*

Institut für Organische Chemie und Makromolekulare Chemie, Universität Düsseldorf, D-4000 Düsseldorf, West Germany

ROBIN WALSH*

Department of Chemistry, University of Reading, WhiteKnights, Reading RG6 2AD, England

Received November 10, 1988 (Revised Manuscript Received May 8, 1989)

Contents

I. Introduction

Among the many families of isomeric strained hydrocarbons, the $(CH)_8$ group is one of the most interesting.[2] This arises, in part, from the size, i.e., the number of members, being large enough to provide considerable variety of behavior but not so large that a coherent picture becomes unachievable. The number of isomers may be determined by graph theory.[3-6] All compounds so far known correspond to planar graphs (i.e., their formulas can be written so that no lines (bonds) are crossing). The possible planar graphs lead to 17 constitutional isomers (a constitutional graph is one whose points symbolize atoms and whose lines symbolize covalent bonds). Including stereoisomers, however, there are 21 isomers in all.[8] So far, 13 of these isomers have been made, and a 14th is crucially implicated in several of the rearrangements. These members of the family are shown in Figure 1 as compounds **1–14**.

This review concentrates on thermal, photochemical, and catalyzed behavior of these 14 isomers. To round out the picture, spectroscopic properties, particularly photoelectron spectra, which reveal the pattern of energy levels, are also included. Other C_8H_8 isomers that are not part of the $(CH)_8$ family are not in general included in this review (to keep the article tractable) but are mentioned where their reactions are relevant. Earlier reviews have dealt with thermal and photochemical rearrangements.[7-10] Noteworthy are those of Scott and Jones[7] and Chapter 8 of Gajewski's book[10] on hydrocarbon thermal isomerizations. Sufficient new data have accumulated since these last reviews to merit a reexamination. New thermal isomerization studies have provided a fairly comprehensive picture of the energy surfaces involved. Moreover, two of these studies reveal the phenomenon of reactions enhanced through vibrational energy release. Kinetic and theoretical modeling of this has been carried out in sufficient detail to merit a special section. There has been some progress in understanding the photochemistry of these hydrocarbons, but in general there remains a considerable lack of detail about the states involved and in some cases still confusion concerning the products.

II. Reactivity of the $(CH)_8$ Hydrocarbons

A. Thermal Behavior

1. Heats of Formation

A proper understanding of the energy hypersurface of the $(CH)_8$ family cannot be obtained without a knowledge of gaseous heats of formation. Experimental values are available in only a few cases. Combustion calorimetry has been used for cubane (**1**),[11] the most strained member of the $(CH)_8$ family, and yields $\Delta H_f^\circ = 148.7 \pm 1.0$ kcal·mol^{-1}. The only other molecule to which this method has been applied is cyclooctatetraene (**13**),[12] giving $\Delta H_f^\circ = 71.1 \pm 0.3$ kcal·mol^{-1}. Heats of catalytic hydrogenation have been determined for **13**[13] and also for barrelene (**11**).[14] When corrected for heats of solution, these lead to $\Delta H_f^\circ(13) = 69.4 \pm 0.3$ kcal·mol^{-1} [15] and $\Delta H_f^\circ(11) = 72.5 \pm 1.5$ kcal·mol^{-1}.[16] Thus for cyclooctatetraene (**13**) there is a small discrepancy that merits further investigation. Equilibrium studies have been or may be used to derive heats of formation.

0009-2665/89/0789-1125$06.50/0

Karin Hassenrück was born in 1960 in Düsseldorf, West Germany. She studied chemistry at Düsseldorf University, where she obtained her Diplom-Chemiker in 1985. She worked on polycyclic molecules with annulated four-membered rings and received her Dr. rer. nat. under the supervision of Hans-Dieter Martin in 1988 at Düsseldorf University. During the time she was a graduate student, she visited Robin Walsh in Reading, England, and Josef Michl in Austin, TX, with a DAAD stipendium. As a postdoctoral fellow she was associated with Josef Michl at the University of Texas at Austin. During this time she received a Feodor-Lynen-Stipendium. She is interested in strained compounds and their properties. Her hobbies are music and hiking.

Hans-Dieter Martin was born in Berlin, studied chemistry in Freiburg i.Br. (West Germany), and received his Diploma and Ph.D. degree (1969) at the University of Freiburg i.Br. under the direction of Professor H. Prinzbach. After 3 years of postdoctoral work at the University of Basel under Professor E. Heilbronner and at the University of Reading under Professor H. M. Frey, he was Professor of Organic Chemistry in Würzburg (1975–1980) and presently is Full Professor of Organic Chemistry in Düsseldorf. His research interests concern carbocyclic and heterocyclic organic compounds, particularly strained molecules, new chromophores for dyes and pigments, and medium-sized heterocycles.

Robin Walsh was born in 1939 in London, England. He studied at Cambridge University, where he obtained his B.A. in 1961 and Ph.D. in 1964. After this he held postdoctoral positions with Sidney Benson at Stanford Research Institute and Monty Frey at the University of Reading, where he joined the staff in 1967. Dr. Walsh's research interest in the broadest sense may be described as quantitative aspects of chemical reactivity. He is a gas-phase kineticist and photochemist but maintains an interest in thermodynamics. He has particular interests in the measurement of bond dissociation energies, the study of strained-ring hydrocarbon rearrangements, and the gas-phase chemistry of silicon-containing species. In 1977, Dr. Walsh spent 6 months in Jurgen Troe's laboratories working on the problem of direct observation of unimolecular reaction of energized molecules. Dr. Walsh was secretary and chairman of the gas kinetics discussion group of the Royal Society of Chemistry between 1979 and 1984. His recreational activities include running half-marathons.

From the temperatue dependence of equilibrium constants ("second-law method") reaction enthalpies were obtained for the equilibrium reactions of cyclooctatetraene (**13**) with both semibullvalene (**10**)[17] and bicyclo[4.2.0]octa-2,4,7-triene (**12**).[18] Assuming negligible *corrections to room temperature (usually a reasonable assumption)* and taking the combustion value for $\Delta H_f°(\mathbf{13})$, one can calculate $\Delta H_f°(\mathbf{10}) = 73.6 \pm 1.0$ kcal·mol^{-1} and $\Delta H_f°(\mathbf{12}) = 76.6 \pm 1.0$ kcal·mol^{-1}. These would be 1.7 kcal·mol^{-1} too high if the alternative, lower value for $\Delta H_f°(\mathbf{13})$ were correct.

The shortage of data and the increasing power of computers have encouraged the growth of semiempirical and ab initio calculations in this area (as for many other substances). In the semiempirical category MINDO calculations[19-21] do not reproduce $(CH)_8$ heats of formation very well, and it is questionable whether MINDO/3[21] is better than MINDO/1,[20] although the values for $\Delta H_f°$ for cubane (139.8[21] and 116.9 kcal·mol^{-1} [20]) do indicate improvement in that case. A newer version of the parameterized quantum mechanical model, AM1,[22] gives better results for cubane, $\Delta H_f°(1) = 151.2$ kcal·mol^{-1}. We have calculated the $\Delta H_f°$ values for the other $(CH)_8$ hydrocarbons using both MNDO and AM1,[97] but the results (Table 1) do not show especially good agreement with experimental values where these are known. In principle, *force field* calculations should be capable of providing very good values for heats of formation in the $(CH)_8$ family, since an extensive data base of dynamic information exists on simpler hydrocarbons, both strained and unstrained.[23,24] The latest version for saturated species,[25] MM2, gives a value of $\Delta H_f° = 148.8$ kcal·mol^{-1} for cubane. A reparameterization of MM2,[26] carried out to improve predictions of internal rotation barriers, leaves $\Delta H_f°(1) = 148.7$ kcal·mol^{-1}, essentially unchanged. The application of MM2 to cuneane (**3**) required another model[27] modified to deal more effectively with linked three-membered rings. This led to $\Delta H_f°(\mathbf{3}) = 110$ kcal·mol^{-1}.[38] In yet another version, MMP1, developed for molecules with double bonds, the value for cyclooctatetraene, $\Delta H_f° = 70.4$ kcal·mol^{-1}, was obtained,[28] in good agreement with experiment. In principle, there is no reason why these models should not give reliable values for all hydrocarbons, although Nature appears to find new difficulties in too many individual cases for comfort.

A more general, slightly less accurate but simpler, approach is to use Benson's group additivity method for strainless compounds[29] and calculate the ring strain energy by summation of contributions of the individual small rings. For example, for cubane

$$\Delta H_f° = 8\Delta H_f°[\text{C}-(\text{C})_3(\text{H})] + 6E(\text{strain}_{\text{cyclobutane}})$$
$$= 8(-1.9) + 6(26.2) = 142.0 \text{ kcal·mol}^{-1}$$

a slight (but not severe) underestimate.

TABLE 1. Experimental and Calculated Heats of Formation (kcal·mol^{-1}) for $(CH)_8$ Hydrocarbons

compd[a]	expt	MINDO/1[b]	MINDO/3[c]	MM2 (MMP1)	additivity[d]	ab initio	MNDO[e]	AM1[e]
1	148.7[f]	116.9	139.8	148.7[g]	142	148.7[h]	99.0[i]	151.2[i]
2		121.0			124		142.9	172.4
3		106.0		110.0[j]	106		100.8	133.9
4		155.0			93		98.8	129.5
5		115.4			115		118.8	149.7
6		95.1			102		96.0	115.7
7		64.8	132.3		81		103.4	125.3
8		120.2	120.2		116		102.5	138.2
9		120.8	123.1		118		105.0	141.7
10	73.6[d,k]	53.0	91.3		70		87.8	99.1
11	72.5[d]	78.0	99.0			76.7[l]	67.5	67.3
12	76.6[d]	77.9	78.4		80		64.2	81.8
13	71.1[m]	66.4	58.1	70.4[n]		69.1[h]	56.2	63.5
14		77.9			95		92.7	118.0

[a] See Figure 1. [b] References 20 and 37. [c] Reference 21. [d] See text. [e] Reference 97. [f] Reference 11. [g] Reference 26. [h] Reference 32. [i] Reference 22. [j] Reference 38. [k] Reference 17. [l] Reference 36. [m] Reference 12. [n] Reference 28.

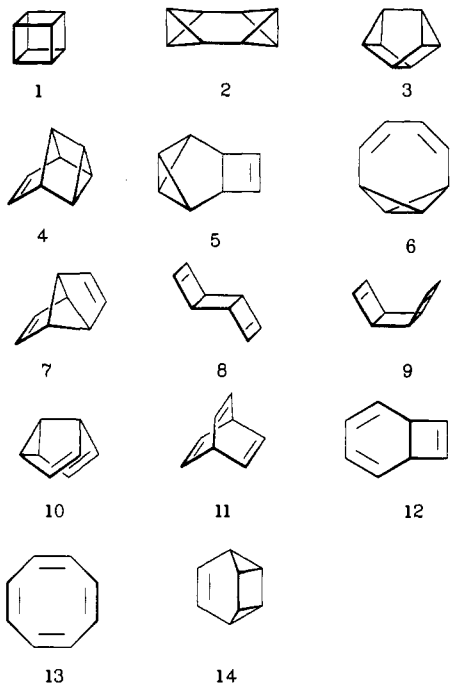

Figure 1. $(CH)_8$ hydrocarbons.

The trouble with this method is the complexity of coupling of ring structures in polycyclic molecules, which leads to special situations (for example, bicyclo[2.2.1]systems). A valiant attempt has been made to allow for these situations,[30] and using this and occasional chemical intuition, we have estimated the heats of formation of most members of the $(CH)_8$ family. The results are shown in Table 1, along with the other data mentioned in this section. This approach appears to underestimate values by ca. 1 kcal·mol^{-1} per small ring (three-, four-, or five-membered ring). Ab initio calculations have now developed to the level where values of chemical accuracy are beginning to emerge. The techniques and procedures are too elaborate to discuss in detail, but the quality of calculation improves with the quality of basis set and the use of electron correlation. Relating ab initio to experimental energies in a way that helps cancel any remaining errors can then be done either by use of iso- or homodesmic reactions[31,32] or by use of atom[33] or group equivalents.[34,35] A calculation at a high level by Disch et al.[32] using a 6-31G* basis at an MP2 level gave $\Delta H_f°$[cyclooctatetraene (13)] = 69.1 kcal·mol^{-1} and $\Delta H_f°$[cubane (1)] = 148.7 kcal·mol^{-1}, using homodesmic reactions to obtain the heats of formation. As a somewhat lower

SCHEME 1

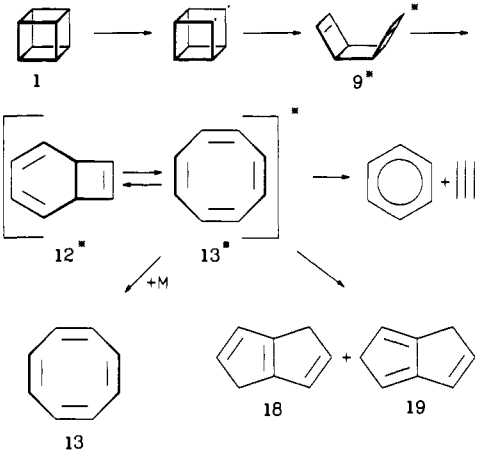

level of calculation an STO-3G basis set at the SCF level[36] using isodesmic reactions (not as good as homodesmic reactions) gave $\Delta H_f°$[barrelene (11)] = 76.7 kcal·mol^{-1}. Wiberg, using group equivalents,[34,35] calculated $\Delta H_f°$[cubane (1)] = 147.1 kcal·mol^{-1} with a 6-31G* basis set. Clearly, the calculations, especially the higher level ones, are good.

However, in spite of all these advances, much remains to be done on the thermochemistry of $(CH)_8$ hydrocarbons. It is our feeling that if a heat of formation is lacking, and a friendly theoretical chemist with a good program is not at hand, group additivity (with additivity of ring strain) will give a value quickly, painlessly, and probably reliable to better than 5 kcal·mol^{-1}.

2. Valence Isomerizations

Cubane (1), the molecule with the highest heat of formation and strain energy, is surprisingly thermally stable. Gas-phase thermolysis at temperatures in excess of 200 °C gives rise to acetylene, benzene, cyclooctatetraene (13), and several dihydropentalenes.[39,40] At high pressures 13 predominates while at low pressures the other products are the main ones. This has been explained[39,40] in terms of the intermediacy of highly vibrationally excited cyclooctatetraene, which can either be stabilized or react further. The mechanism is shown in Scheme 1.

The first step involves single C–C bond breaking to form a biradical that then breaks a further bond to form 9*, which is too vibrationally excited to be stabilized. 9* then leads via 12* to 13*, all known rearrangements. The stability of cubane is explained by Martin et al.[39,40] by the fact that the biradical formed in the rate-de-

SCHEME 2

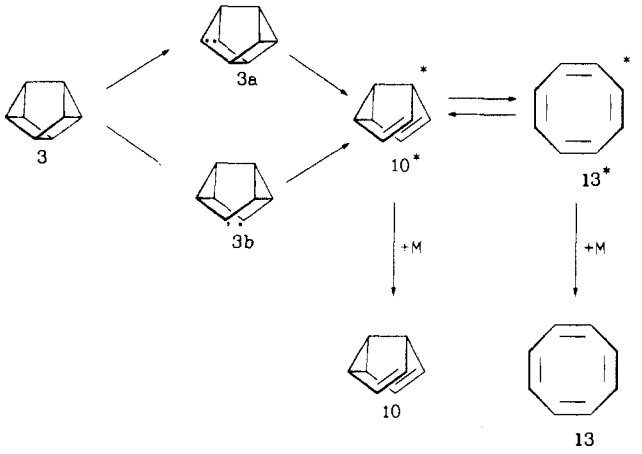

termining step still has its molecular cage largely intact, and its formation, therefore, offers little by way of strain release. An alternative explanation in terms of a concerted forbidden process (in the Woodward–Hoffmann sense) leading from 1 to 9* has been offered by Doering et al.[41] It may be rather difficult in practice to distinguish such alternatives, but in any case the biradical intermediate is energetically accessible. Kinetic studies of cubane pyrolysis in the temperature range 230–260 °C show first-order behavior and give the Arrhenius equation

$$\log (k/s^{-1}) = (14.68 \pm 0.44) - (43.1 \pm 1.0 \text{ kcal·mol}^{-1})/RT \ln 10 \quad (1)$$

Further discussion of the pressure dependence appears in the next section.

There has been no report of the thermolysis of octabisvalene (2). Cuneane (3) is another molecule with a very high strain energy, but again, like cubane, it is surprisingly stable, not decomposing substantially below 180 °C. Gas-phase thermolysis produces semibullvalene (10) and cyclooctatetraene (13) in proportions that are pressure dependent, with 10 predominating at high pressures and 13 at low pressures.[38] This has been explained by the involvement of vibrationally excited semibullvalene (10*) reacting reversibly to form vibrationally excited cyclooctatetraene (13*). The mechanism is shown in Scheme 2.

The initial step is single C–C bond breaking in the most strained part of the molecule, but there are two possibilities leading to either biradical 3a or 3b. The authors,[38] while preferring the pathway via 3b, were unable to rule out 3a. Both biradicals are energetically accessible on the basis of the measured activation energy. Kinetic studies[38] in the temperature range 230–260 °C show first-order behavior and give the Arrhenius equation

$$\log (k/s^{-1}) = (13.82 \pm 0.09) - (37.7 \pm 0.2 \text{ kcal·mol}^{-1})/RT \ln 10 \quad (2)$$

As with cubane, the initially formed biradical, whether 3a or 3b, retains a substantial degree of ring strain and this accounts for the surprising stability of 3. However, once a second bond in the biradical is broken, sufficient energy is released to form semibullvalene (10*) in a highly vibrationally excited state. Further discussion

SCHEME 3

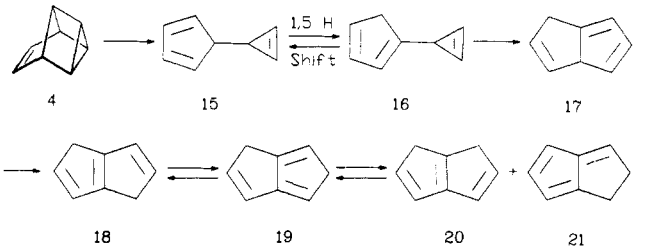

SCHEME 4

of this and the pressure dependence of product formation in cuneane (3) pyrolysis appears in the next section.

Thermolysis of tetracyclo[3.3.0.$0^{2,4}$.$0^{3,6}$]oct-7-ene (4) in a flow system (temperatures > 200 °C), studied by Stapersma et al.,[42,43] gives a mixture of products that are subject to rapid polymerization and isomerization. These were identified as dihydropentalenes 18, 19, 20, and 21 by trapping experiments with $F_3CC{\equiv}CCF_3$. Independent experiments showed that 19 isomerized to the same mixture under the conditions of pyrolysis. Semibullvalene (10) and cyclooctatetraene (13), however, were notably absent under temperature conditions at which they are stable. The authors proposed the mechanism in Scheme 3.

The initial, rate-determining step is a retro-Diels–Alder reaction giving dihydrocalicene (15), which rearranges via a 1,5-hydrogen shift to 16 and thence to dihydropentalene (17) by an analogue of the vinylcyclopropene–cyclopentadiene rearrangement. 17 rapidly isomerizes again via 1,5-hydrogen shifts to the observed dihydropentalenes 18, 19, and 20. This dihydropentalene mixture, in which 1,5-dihydropentalene (19) is the most abundant and therefore most stable component, is formed in the pyrolyses of a number of $(CH)_8$ hydrocarbons[40,45,72] and has been investigated by Meier and co-workers.[44,46,47] Five of the dihydropentalenes can readily and rapidly interconvert at low temperatures via 1,5-hydrogen shifts, but a sixth isomer, 1,2-dihydropentalene (21), cannot be generated by this route. It is, however, sufficiently stable to be observed in the thermolysis of 4 and other $(CH)_8$ hydrocarbons. Evidence from cyclooctatetraene (13) pyrolysis suggests its formation from other dihydropentalenes is not unimolecular but rather catalyzed.

In the rearrangement of 4, all proposed intermediates (i.e., 15, 16, and 17) are known or plausibly argued to rearrange too rapidly to be observed under thermolysis conditions. The intermediacy of the bicyclo[3.3.0]-octa-2,6-diene-4,8-diyl biradical (22, Scheme 4) was ruled out[43] by the absence of 10 or 13 among the products. Lack of scrambling in appropriately D-labeled versions of 4 was argued to rule out a two-step formation of 15 via biradical 23 on the grounds that formation of 23 from 4 should be reversible.

Kinetic studies have not been carried out but from the conditions of study we may estimate an activation energy of 38 (±3) kcal·mol^{-1}. This could make biradical 23 energetically accessible, although uncertainties are large.[48] Finally, it is worth noting that in the decom-

SCHEME 5

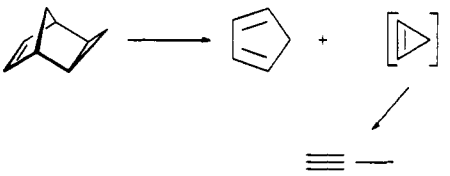

SCHEME 5a

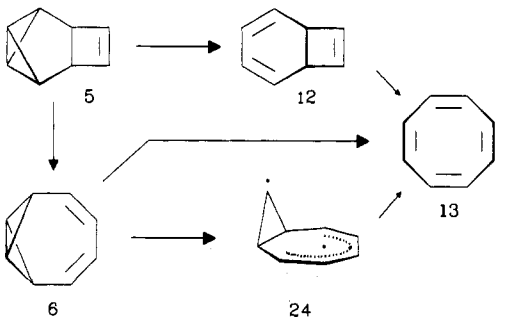

SCHEME 6

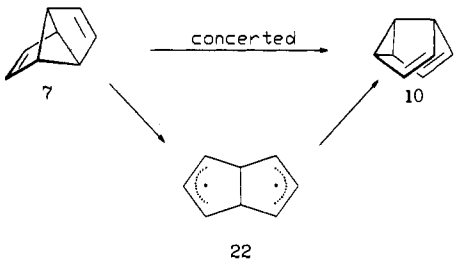

position of *exo*-tricyclo[3.2.1.$0^{2,4}$]oct-6-ene[49] (Scheme 5), the analogous retro-Diels–Alder reaction does occur as a minor pathway.

The pyrolyses of both tetracyclo[4.2.0.$0^{2,4}$.$0^{3,5}$]oct-7-ene (**5**)[50] and octavalene (tricyclo[5.1.0.$0^{2,8}$]octa-3,5-triene) (**6**)[51] apparently both lead to cyclooctatetraene (**13**). **5** rearranges in the gas phase above temperatures of ca. 250 °C although in solution, while it is claimed to rearrange at 140 °C in chloronaphthalene, it does not do so in benzene for as long as 2 days. Catalysis is suspected in chloronaphthalene. **6** is much less stable and rearranges slowly at 80 °C ($CDCl_3$ solution). It is not certain that this is a unimolecular pathway, as catalysis by traces of acid could not be ruled out. Possible mechanisms are included in Scheme 5a.

For **5** the question is whether the bicyclo[1.1.0]butane or cyclobutene portion of the molecule rearranges more rapidly while for **6** the choice of pathways seems to lie between a direct concerted process and one involving the highly stabilized biradical **24**. No kinetic data are available.

The thermal rearrangement of tricyclo[3.3.0.$0^{2,6}$]-octa-3,7-diene (**7**) occurs readily at room temperature[52-54] to give semibullvalene (**10**). Both reactant decay and product growth were observed in CCl_4 solution by NMR. Both concerted[55,56] and two-step mechanisms[10,54,57] have been proposed (Scheme 6). The latter involves the intermediacy of the bicyclo[3.3.0]-octa-2,6-diene-4,8-diyl biradical (**22**). Although kinetic studies have not been carried out, Frey and Hopkins[57] have estimated the following Arrhenius equation (by comparison with tricyclo[3.3.0.$0^{2,6}$]oct-3-ene pyrolysis):

$$\log (k/s^{-1}) = 14.0 - (22.8 \text{ kcal·mol}^{-1})/RT \ln 10 \quad (3)$$

which corresponds to a lifetime of ca. 10 min for **7** at

SCHEME 7

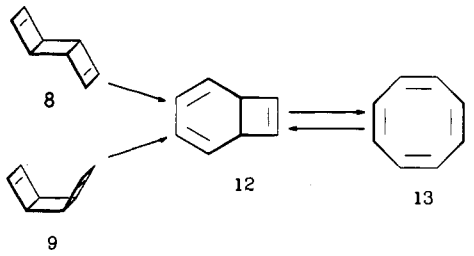

20 °C. From our estimated heat of formation of **7**, this implies a transition-state energy of ca. 104 kcal·mol^{-1}, about 9 kcal·mol^{-1} greater than that of **22**,[17] making the biradical **22** energetically accessible. In spite of the uncertainties of such estimates (probably ca. ±5 kcal·mol^{-1}), this strongly argues in favor of the two-step mechanism. The proposed concerted mechanisms, involving antarafacial components, look to involve extremely difficult geometric contortions of **7**. The most likely concerted mechanism would appear to involve a forbidden suprafacial 1,3-carbon shift across one of the π-allylic components of **7**. The fact that **7** does not rearrange to cyclooctatetraene (**13**) has been attributed to the forbidden character of the reaction,[10,54] but it may equally be argued that biradical **22** collapses to semibullvalene (**10**) more readily than to **13** for reasons of strain. This point is taken further in the discussions of semibullvalene (**10**) and cyclooctatetraene (**13**) pyrolyses.

The syn and anti dimers of cyclobutadiene were first synthesized in 1964 and thermolyzed in dichlorobenzene solution at 140 °C to give cyclooctatetraene (**13**).[59] Kinetic studies have been carried out by two groups,[60,61] and the decompositions show first-order behavior. Frey, Martin, and Hekman[60] obtained the following Arrhenius equations:

$$\log (k(8)/s^{-1}) = (14.01 \pm 0.09) - (32.59 \pm 0.17 \text{ kcal·mol}^{-1})/RT \ln 10 \quad (4)$$

$$\log (k(9)/s^{-1}) = (14.22 \pm 0.09) - (30.49 \pm 0.16 \text{ kcal·mol}^{-1})/RT \ln 10 \quad (5)$$

Very similar equations were obtained by Dewar et al.[61] **9** decomposes faster than **8** undoubtedly because of the greater ground-state steric strain of the syn isomer. Both these reactions are forbidden (in the Woodward–Hoffmann sense) and probably proceed via the intermediacy of bicyclo[4.2.0]octa-2,4,7-triene (**12**) (Scheme 7). The formation of **12** itself involves a forbidden [π2s + σ2s] pathway but is probably concerted by analogy with the decomposition of bicyclo[2.2.0]hex-2-ene.[62,63] If a biradical were involved here, it would be difficult to distinguish it from an excited state of **12**. Nevertheless both a biradical and a triplet-state pathway have been discussed.[60,61]

Semibullvalene (**10**), discovered by Zimmerman and Grunewald,[64] is remarkable for the rapidity of its degenerate Cope rearrangement, which takes place at −150 °C, with an activation energy 4.8 ± 0.2 kcal·mol^{-1} in CF_2Cl_2 solution[65] (^{13}C NMR: 5.24 ± 0.09 kcal·mol^{-1}).[65a] The degeneracy of the rearrangement is removed in the solid state, probably by intermolecular perturbations, although the rearrangement (exothermic direction) re-

SCHEME 8

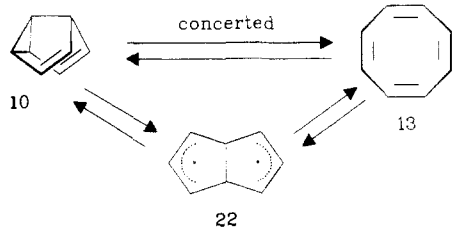

mains essentially as fast as in solution.[66,67] Numerous theoretical calculations[68-71] show that this reaction is one of the archetypal concerted processes, although estimates of the activation energy vary considerably according to the quality (level) of the calculation. The best calculation, giving an activation energy of 5.7 kcal·mol^{-1} (MNDO + CI), would appear to be that of Miller et al.[70] The small size of the activation barrier continues to excite the possibility that, by suitable substitution, the transition-state bishomobenzene structure can be stabilized relative to the classical semibullvalene.[70,71] This remains a challenge for experimentalists.

The high-temperature thermolysis of semibullvalene (**10**) appeared for a while controversial in that different groups claimed to observe different products.[43,58,72] Two studies (250–300 °C) using flow pyrolysis (with NMR analysis of products) claimed cyclooctatetraene (**13**) was the sole product[43,58] whereas another using a shock tube (470–630 °C) and UV monitoring suggested 1,5-dihydropentalene as the main product.[72] This has been resolved in a quantitative study[17] of the kinetics (static system, GC analysis) that showed unequivocally that **13** was the only product in the temperature range 200–360 °C. The reaction was found to be reversible, with equilibrium quantities of **10** lying in the range 2–4% at temperatures of 270–360 °C. Both forward and reverse reactions were first order and the following Arrhenius equations were obtained:

$$\log (k(\mathbf{10}\rightarrow\mathbf{13})/\mathrm{s}^{-1}) = (13.81 \pm 0.08) - (39.82 \pm 0.19\ \mathrm{kcal\cdot mol^{-1}})/RT \ln 10 \quad (6)$$

$$\log (k(\mathbf{13}\rightarrow\mathbf{10})/\mathrm{s}^{-1}) = (13.15 \pm 0.08) - (42.19 \pm 0.19\ \mathrm{kcal\cdot mol^{-1}})/RT \ln 10 \quad (7)$$

Other nonkinetic studies show interconversions of the tetramethyl- and octamethyl-substituted versions of **10** and **13**, with equilibrium lying more in favor of the semibullvalene.[73,74] Both concerted (2s + 2a + 2a) and two-step mechanisms have been proposed, but our calculations[17] show that the biradical intermediate **22** is energetically accessible and therefore likely to be involved (Scheme 8).

Since the study of **7** showed that the probable intermediate is also the biradical **22**, clearly this must preferably close to **10** rather than open to **13**. Thus central bond breaking in **22** is the rate-determining step in the interconversion of **10** to **13**. The bicyclo[3.3.0]-octa-2,6-diene-4,8-diyl biradical (**22**) plays a key role in several of the $(CH)_8$ rearrangements. From the various kinetic studies reviewed here together with thermochemical estimates a selected portion of the energy surface may be constructed as shown in Figure 2. Further discussion of the involvement of **22** is given later in the section on the pyrolysis of cyclooctatetraene (**13**). It is worth mentioning, however, that **22** is a rather unusual biradical in that it is in part delocalized but geometric constraints force the two allylic fragments together. Its energy is estimated[17] in the usual way by assuming no significant interaction between radical centers. In this sense it corresponds to an excited state of bishomobenzene in which the wave function has a nodal plane parallel to and encompassing the bridgehead C–C bond.

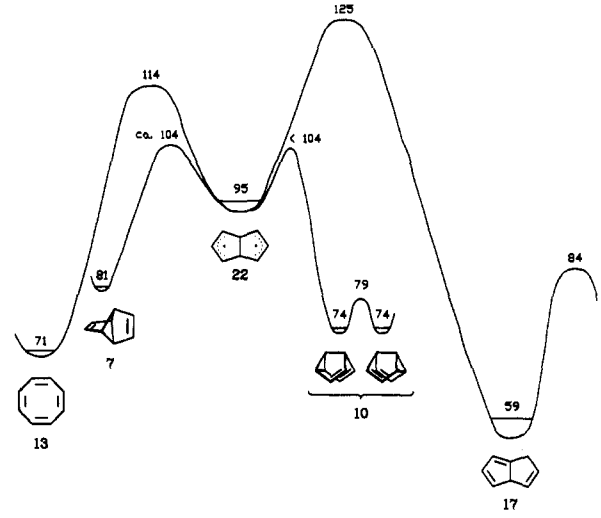

Figure 2. Energy surface of selected $(CH)_8$ hydrocarbons. Energies in kcal·mol^{-1}. See text for details.

SCHEME 9

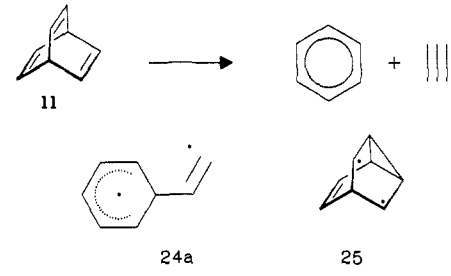

The pyrolysis of barrelene (bicyclo[2.2.2]octa-2,5,7-triene (**11**)) has been studied between 210 and 250 °C.[16] The products are benzene and acetylene in equal amounts. The kinetics are first order and the reaction is homogeneous and unimolecular. The rate constants fit the Arrhenius equation

$$\log (k/\mathrm{s}^{-1}) = (14.27 \pm 0.18) - (41.71 \pm 0.41\ \mathrm{kcal\cdot mol^{-1}})/RT \ln 10 \quad (8)$$

These Arrhenius parameters are consistent with a concerted retro-Diels–Alder process. Thermochemical estimates rule out the involvement of biradicals **24a** and **25** (Scheme 9).

Bicyclo[4.2.0]octa-2,4,7-triene (**12**) is a valence tautomer of cyclooctatetraene (**13**) and is in rapid equilibrium with it at room temperature. By an indirect trapping method, Huisgen[75] estimated that roughly 0.01% of **12** was present in **13** at 100 °C. More recently, the equilibrium has been studied directly between 400 and 700 °C by freezing the mixture from the gas phase onto a cold surface and analyzing by NMR at −40 °C.[18] The thermodynamic parameters of this equilibrium were measured,[18] and we have used the $\Delta H°$ to obtain

SCHEME 10

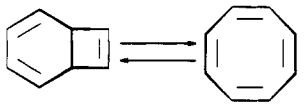

12 13

$\Delta H_f°$ for **12** (see section on heats of formation). Kinetic studies of the reaction **12** → **13** were carried out in solution by Vogel et al.[75a] between −20 and 0 °C using NMR. These gave the Arrhenius equation

$$\log (k/s^{-1}) = (11.96 \pm 0.66) - (18.7 \pm 0.8 \text{ kcal·mol}^{-1})/RT \ln 10 \quad (9)$$

Combination of this equation with the thermodynamic data allows us to calculate the Arrhenius equation for **13** → **12**:

$$\log (k/s^{-1}) = 11.02 - (24.2 \text{ kcal·mol}^{-1})/RT \ln 10 \quad (10)$$

This reaction (Scheme 10) undoubtedly is an allowed (2s + 2s + 2s) concerted electrocyclic reaction. The *A* factors of eq 9 and 10 look slightly low compared with those of the semibullvalene (**10**) ⇌ cyclooctatetraene (**13**) equilibrium,[17] in spite of mechanistic differences. The interconversion activation energies for **12** and **13** should probably be ca. 2 kcal·mol^{-1} higher than those of eq 9 and 10.

Of all the $(CH)_8$ hydrocarbons cyclooctatetraene (**13**) justifiably lays claim to being both the most versatile and the most fascinating. Already known for nearly 80 years,[76] the processes of its thermal behavior are still in the process of clarification. Three temperature regimes may be used to delineate its behavior. At low temperatures (<100 °C) the processes of ring inversion and bond switching occur. These are discussed by Gajewski[10] and the discussion is not repeated in detail here. The ring-inversion process occurs through a planar transition state with an activation in the range 12–15 kcal·mol^{-1}. Ab initio calculations predict a value of 17.8 kcal·mol^{-1}.[77] The bond-switching process also occurs via a planar intermediate, although its rate appears to be slightly slower. Recent measurements of the kinetics by dynamic NMR line-shape analysis in nematic-phase solvents[78] using a spectral line-shape simulation technique gave the Arrhenius equation

$$\log (k/s^{-1}) = 10.85 - (10.62 \text{ kcal·mol}^{-1})/RT \ln 10 \quad (11)$$

The *A* factor of this process is low in terms of transition-state theory but may be affected by either solvent effects or heavy-atom tunneling. The activation energy is probably lower than the classical barrier. Substituents considerably raise the barrier to bond switching.[10] The reversible valence isomerization to bicyclo[4.2.0]-octa-2,4,7-triene (**12**), already discussed, is a further low-temperature process.

The medium-temperature regime may be classified as 100–400 °C. In this region the reversible valence isomerization to semibullvalene (**10**), already described, takes place. Also operative in this region is another degenerate rearrangement leading to carbon scrambling in the cyclooctatetraene ring. This process has been elucidated by Paquette et al.[79] and is again described in some detail by Gajewski.[10] The available evidence

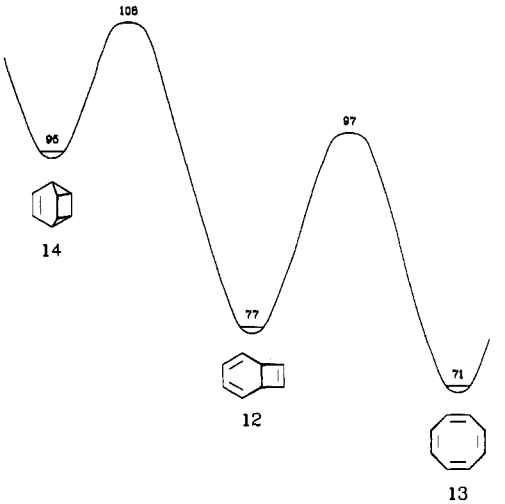

Figure 3. Energy surface of selected $(CH)_8$ hydrocarbons. Energies in kcal·mol^{-1}. See text for details.

SCHEME 11

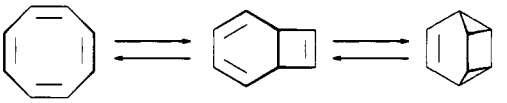

13 12 14

(methyl-shift processes) points to the involvement of tetracyclo[4.2.0.0^{2,8}.0^{5,7}]octene (**14**), a $(CH)_8$ isomer that although often discussed[37] has not thus far been isolated. Its formation comes about from intramolecular Diels–Alder cycloaddition from bicyclo[4.2.0]octa-2,4,7-triene (**12**) (Scheme 11).

The kinetics of this process have not be investigated but from the flow system conditions used by Paquette, Gajewski[10] estimated $\Delta G^{\ddagger}$ in the range 42–47 kcal·mol^{-1}. From the likely tight transition state for formation of **14** from **13**, we may estimate an *A* factor of $10^{11.5}$ s^{-1} and an activation energy of 37 ± 3 kcal·mol^{-1}. From this value and others already mentioned, together with thermochemical estimates from Table 1, another portion of the energy surface may be constructed as shown in Figure 3. It is clear from the figure that **14** is extremely kinetically unstable, with an activation energy of only ca. 13 kcal·mol^{-1} toward decomposition. Evidently a successful synthesis will require very low temperatures.

The high-temperature regime for cyclooctatetraene (**13**) pyrolysis may be classified as temperatures in excess of 400 °C. Of course, the low- and medium-temperature studies imply that at high temperatures equilibrium amounts of **12** and **10** will necessarily be present in **13**. In practice, these are so small that effectively the bulk reactant is mainly **13** (≥96%). Flow pyrolyses (with GC detection of products)[72,80,81] reveal the presence of acetylene, benzene, 1,5-dihydropentalene (**19**), and styrene at temperatures below 750 °C and further (mainly aromatic) products at even higher temperatures. A shock tube kinetic study[72] between 1000 and 1400 K with IR and UV analysis of products suggested two independent, unimolecular pathways (Scheme 12). Arrhenius equations (12) and (13) were obtained for these processes:

$$\log (k_a/s^{-1}) = 12.6 - (45.9 \text{ kcal·mol}^{-1})/RT \ln 10 \quad (12)$$

$$\log (k_b/s^{-1}) = 13.8 - (53.5 \text{ kcal·mol}^{-1})/RT \ln 10 \quad (13)$$

SCHEME 12

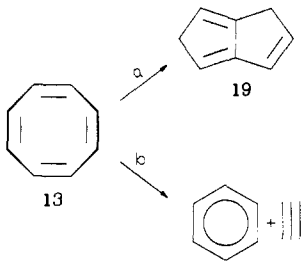

SCHEME 13

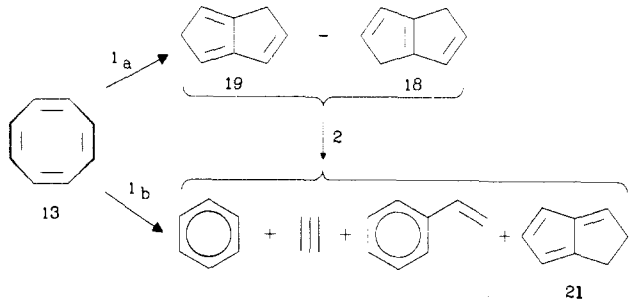

Both these rate constants are acknowledged to be pressure dependent and therefore in the fall-off region of unimolecular behavior.

In a more recent study[45,82] we have confirmed, using static bulb pyrolysis (free from fall-off effects) with GC analysis, that two unimolecular pathways exist and made a more detailed kinetic analysis as shown in Scheme 13. The dihydropentalene pathway (1a) produces both 1,5-dihydropentalene (**19**) and 1,4-dihydropentalene (**18**) as primary products. The ratio is similar to that found in the pyrolyses of **4** and **1** and consistent with the equilibrium study of Meier.[46,47] Pathway 1b produces benzene and acetylene initially but as time elapses styrene and 1,2-dihydropentalene are also formed. These products all accumulate at the expense of **19** and **18**, suggesting an effective channel 2. Kinetic analysis in the temperature range 320–410 °C of the initial rates obtained by extrapolation gave the following Arrhenius equations:

$$\log (k_{1a}/s^{-1}) = (14.16 \pm 0.08) - (54.32 \pm 0.25 \text{ kcal·mol}^{-1})/RT \ln 10 \quad (14)$$

$$\log (k_{1b}/s^{-1}) = (15.51 \pm 0.26) - (59.87 \pm 0.78 \text{ kcal·mol}^{-1})/RT \ln 10 \quad (15)$$

The data were not consistent with a unimolecular reaction for pathway 2 and suggested instead a surface-catalyzed mechanism.

The detailed mechanisms of steps 1a and 1b, as originally proposed by Jones and Schwab,[81] are almost certainly those in Scheme 14. Biradical intermediates **22** and **24a** are both energetically accessible.[45] In fact, for pathway a the surprise is that the rate-limiting barrier is some 30 (±4) kcal·mol^{-1} higher than **22**. From the lower temperature interconversion of **13** and **10** this barrier must be associated with the 1,2-hydrogen shift from **22** leading to 1,8-dihydropentalene (**17**). As has been pointed out before,[43] this is an astonishingly high

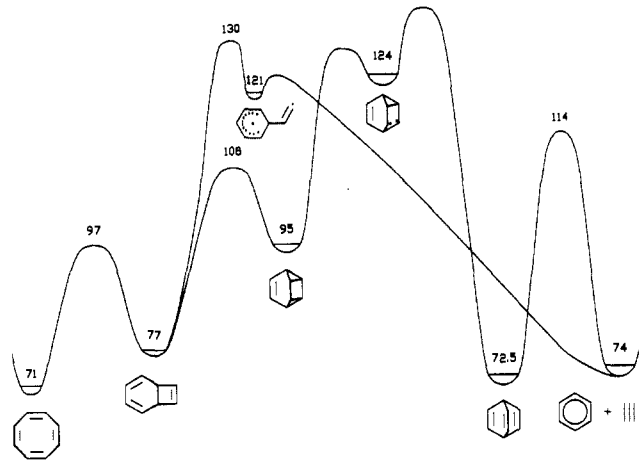

Figure 4. Energy surface of selected $(CH)_8$ hydrocarbons. Energies in kcal·mol^{-1}. See text for details.

SCHEME 14

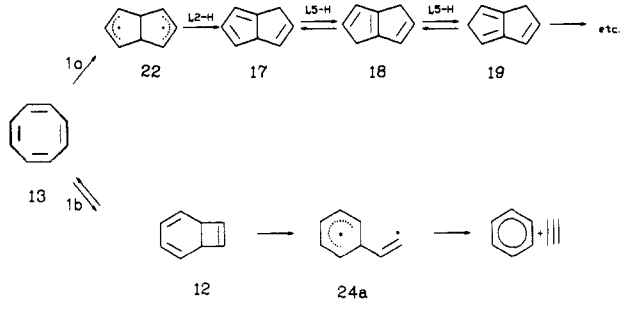

SCHEME 15

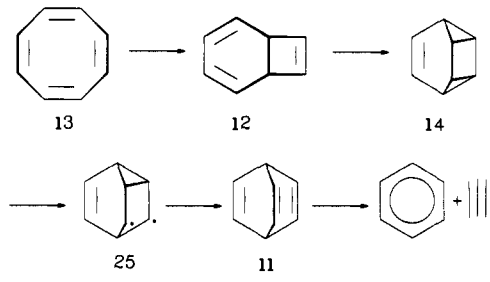

barrier for such a process, which has a magnitude of only a few kcal·mol^{-1} in the prototype 1,3-trimethylene biradical. Probably this hydrogen shift is made difficult both by the rigidity of the molecular frame and by the double allylic character of the biradical. Parts of the relevant energy surface are shown in Figure 2.

For pathway 1b, **24a** is an obvious intermediate and is close in energy to the rate-limiting barrier, which is probably the C–C bond-breaking step from **12**. An alternative mechanism could be via **14**, biradical **25**, and barrelene (**11**) (Scheme 15). Although energetically possible,[45] the high observed *A* factor for reaction 1b is more consistent with the original proposal than this mechanism. This part of the rearrangement energy surface for cyclooctatetraene (**13**) and related $(CH)_8$ isomers is shown in Figure 4, an extension of Figure 3.

The mechanism of formation of styrene and 1,2-dihydropentalene, while apparently surface catalyzed in static bulb experiments, may nevertheless have contributing unimolecular pathways at higher temperatures. Both products appear to be secondary in nature starting from cyclooctatetraene and therefore are probably only formed from the other dihydro-

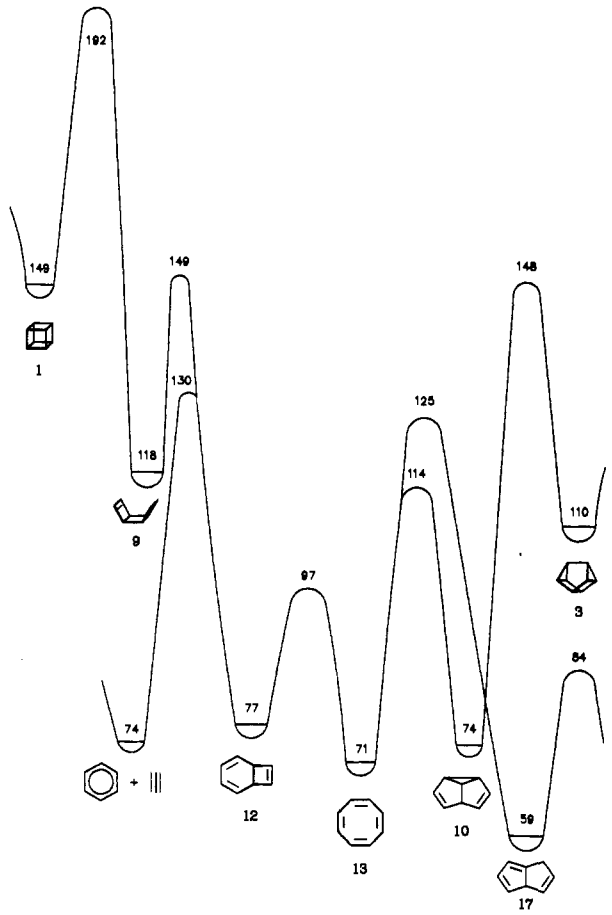

Figure 5. Energy surface of selected $(CH)_8$ hydrocarbons. Energies in kcal·mol^{-1}. Diradical intermediates are omitted. See text for details.

SCHEME 16

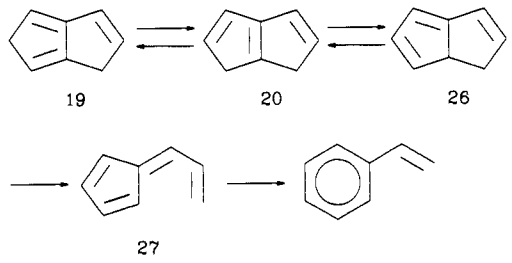

pentalenes. 1,5-Dihydropentalene is thought to rearrange mainly to styrene.[72] A shock tube kinetic study using UV monitoring gave the Arrhenius equation

$$\log (k/s^{-1}) = (13.1 \pm 0.3) - (57.8 \pm 2 \text{ kcal·mol}^{-1})/RT \ln 10 \quad (16)$$

A possible mechanism would be Scheme 16. In this process the rapid 1,5-hydrogen shifts equilibrating the dihydropentalenes mean that any accessible route from one of them will deplete them all. In this case 1,7-dihydropentalene (**26**) can rearrange readily and almost certainly reversibly to 6-vinylfulvene (**27**), which can then form styrene by aromatization of the fulvene moiety. The possible unimolecular mechanism of involvement of 1,2-dihydropentalene (**21**) remains obscure.

A final potential energy surface that emphasizes the key role of cyclooctatetraene (**13**) as product of the rearrangements of **1**, **3**, **9**, **10**, and **12** is shown in Figure 5. In order to simplify this surface biradical intermediates are omitted. This surface helps explain the substantial vibrational energy release that occurs when the energy-rich molecules cubane (**1**) and cuneane (**3**) decompose.

SCHEME 16a

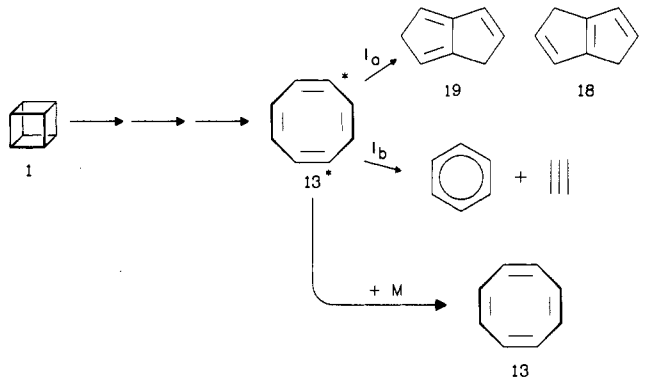

3. *Vibrational Energy Release and RRKM Calculations*

There are relatively few known examples of polyatomic molecule thermolyses resulting in sufficient vibrational energy release to cause further chemical reactions.[83-85]

Because of their high strain energies two members of the $(CH)_8$ family, cubane (**1**) and cuneane (**2**), offer good examples of this phenomenon. In the studies of **1** and **3** carried out in our laboratories[38,40] and discussed in the previous section, conditions for investigation of this phenomenon were particularly favorable. Over the practically accessible pressure range (a few Torr up to nearly 1 atm), the competition between collisional stabilization and further reaction of vibrationally excited products (hot molecules) was balanced in such a way that interception of anywhere between ca. 0 and 90% of hot molecules could be achieved. Thus these systems yield rate constants for reaction of vibrationally excited molecules over quite a wide pressure range and offer excellent possibilities of tests of the theory of unimolecular reactions. We have carried out such tests.[86] Only an outline of the results can be given in the limited space of this review. It turns out that, because of the number of parameters required in such calculations, the theory itself has to be assumed and the calculations have to be limited to verification of some of the parameters. Nevertheless, useful information has been obtained.

Details of the application of RRKM theory to the calculation of rate constants for "chemically activated" molecules using multistep collisional deactivation models can be found in Holbrook and Robinson[87] as well as other texts. In outline, the stages involved are (i) the estimation of the energy, E(initial), or energy distribution of the vibrationally excited species (this can be obtained from the potential energy surface); (ii) the construction of transition-state models for each decomposition pathway of the vibrationally excited species (consistent with measured Arrhenius parameters); and (iii) the calculations of $k(E)$, the energy-specific rate constant, and of $f(E)$, the steady-state fractional population energy distribution, at each particular pressure (or collision frequency) (this depends on the choice of collisional deactivation model and in particular on the average energy removed in a down collision, $\langle \Delta E \rangle_d$; the rate constant at each pressure, k^*, is then obtained as

the sum $\sum k(E)f(E)$ over the effective energy range).

Our findings were as follows:

Cubane (1) System. The decomposition mechanism may be represented by a simplified version of Scheme 1, viz., Scheme 16a. The vibrationally excited molecule is cyclooctatetraene (**13**). Its initial energy distribution was first estimated for the potential energy surface in Figure 5 (and a knowledge of thermal energies) by assuming no losses occurred en route via collisions at intermediate stages, **9** and **12**. This gave a minimum E(initial) of 122 kcal·mol^{-1} and a maximum population of **13*** at ca. 130 kcal·mol^{-1} above the ground state. These energies are well above the barriers for reaction via pathways 1a and 1b. Transition-state models were based on measured Arrhenius parameters.[40,45] The vibrational assignments of the activated complexes for both pathways were made in the usual way by suitable modification of ground-state vibrational wavenumbers after allowance for path degeneracy. No rotational or centrifugal effects were incorporated since geometry changes in the transition states were thought unlikely to affect moments of inertia significantly. The RRKM calculations based on these parameters proved unsatisfactory in that to obtain some kind of a fit required a collisional deactivation model with $\langle \Delta E \rangle_d \approx 4000$ cm^{-1} for c-C_4F_8 as bath gas and $\langle \Delta E \rangle_d \approx 2000$ cm^{-1} for N_2 as bath gas (c-C_4F_8 and N_2 were chosen for these experiments as representative "strong" and "weak" collision partners). Although our knowledge of collisional deactivation efficiencies is far from complete, current evidence from experiments on molecular systems similar to those described here[88-90] suggests values for $\langle \Delta E \rangle_d$ of ca. 1000 (±500) cm^{-1} for c-C_4F_8 and ca. 250 (±100) cm^{-1} for N_2. With these values (and a stepladder deactivation model) reasonable fits were obtained by adjustment of the initial energy distribution minimum (E(initial)) to ca. 105 kcal·mol^{-1} for c-C_4F_8 bath gas and ca. 99 kcal·mol^{-1} for N_2 bath gas. It is doubtful whether the differences in E(initial) are significant. This implies that the reacting cyclooctatetraene (**13**) molecules possess 20 ± 3 kcal·mol^{-1} less energy than the maximum available. This points to the likelihood of losses in energy prior to the formation of **13***. There is some evidence from higher than expected yields of **13** at higher pressures that collisional stabilization of vibrationally excited **9** occurs to a small extent. This interpretation assumes that no other source of error exists. Another possibility could have been the Arrhenius parameters (and dependent transition-state models) for decomposition of **13**. However, other evidence[86] supports the measured Arrhenius parameters.[45] The calculations agree well with the observed product channel ratio, $k_{1b}^*/k_{1a}^* = 3.5 \pm 1.0$ for both bath gases, virtually over the whole pressure range. This ratio was found to be a sensitive function of thermal A factors, requiring a value for A_{1b}/A_{1a} of ca. $10^{1.1}$ (cf. observed value $10^{1.3\pm0.3}$). This is all the more striking in that under thermal decomposition conditions[45] the ratio $k_{1b}/k_{1a} = 0.33$. In other words, the RRKM calculations predict the interchange of major and minor products in going from thermal to chemical activation conditions. Another feature of these calculations is that they also predict the low-pressure "turn-up" phenomenon,[87] characteristic of weak collisional deactivation (as observed).

SCHEME 17

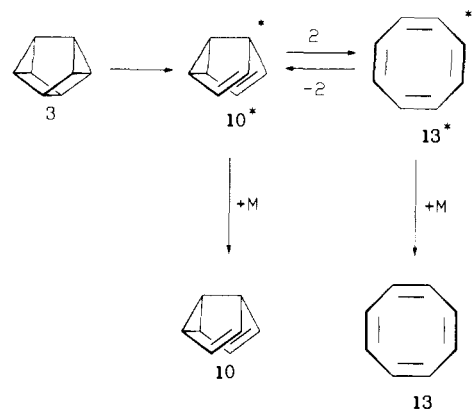

Finally, it was shown that the same transition-state models reproduced quite well the unimolecular fall-off observed by Dudek et al.[72] in their shock tube study of the decomposition of cyclooctatetraene (**13**).

Cuneane (3) System. The decomposition mechanism may be represented by a modified version of Scheme 2, viz., Scheme 17. The initially formed vibrationally excited molecule is semibullvalene (**10**). Its initial energy distribution was estimated from the potential energy surface in Figure 5 to be at least 74 kcal·mol^{-1}. Allowance for the thermal distribution of energies above this gave a maximum population of **10*** at ca. 80 kcal·mol^{-1} above the ground state. This energy is well above the barrier for isomerization to cyclooctatetraene (**13**). The transition-state model was based on measured Arrhenius parameters.[38] As with the RRKM modeling of cyclooctatetraene decomposition, the activated complex was assigned by modification of vibrational wavenumbers (which themselves had to be estimated for ground-state **10**) with allowance for path degeneracy. The first calculations were based on *irreversible* isomerization of **10*** to **13*** via step 2. The RRKM calculations, again performed in combination with a weak collisional (stepladder) deactivation model, gave an approximate fit to the data with $\langle \Delta E \rangle_d = 750$ cm^{-1} for c-C_4F_8 as bath gas and $\langle \Delta E \rangle_d = 310$ cm^{-1} for N_2 as bath gas. These values, as already indicated, are reasonable and suggest that unlike cyclooctatetraene (**13***) formed from cubane (**1**) the semibullvalene (**10***) formed from cuneane (**3**) has the expected energy content. This is consistent with its formation as the *first* product of cuneane (**3**) isomerization. The good fit to the data also suggests that the activated complex assignment (and therefore the thermal Arrhenius parameters) are reasonable.

One feature, however, was poorly fitted, and that was the nonzero (ca. 17–18%) yield of semibullvalene (**10**) at low pressures. In order to match this, reaction 2 was made reversible (i.e., step −2 was introduced). k_{-2}^* was arbitrarily adjusted and the best fit was obtained with k_{-2}^*/k_2^* ca. 0.2. Independent RRKM calculations on step −2 showed that in the energy range of reacting molecules the expected value for $k_{-2}^*/k_2^* = 0.10$. This value, while not in perfect agreement with the best fit to experiments, nevertheless offers reasonable evidence in support of the closeness of **10** and **13** in ground-state energy. This to our knowledge is the first example of a collisionally quenched *reversible* reaction. The observed ratio of rate constants represents a frozen "equilibrium" at that energy above the isomerization

SCHEME 18

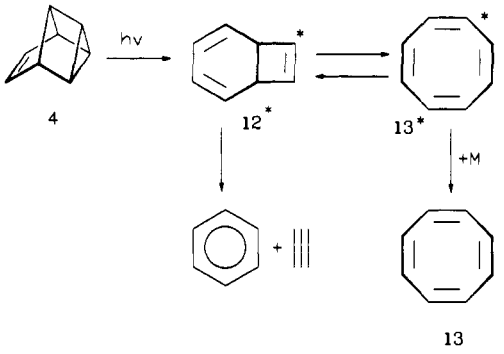

barrier from which the final effective deactivating step takes place. It is a measure of the ratio of state densities at this energy. Finally, it is worth noting that the excess energies involved in forming **13*** from cuneane (**3**) are insufficient to cause reaction to dihydropentalenes (step 1a) or benzene and acetylene (step 1b). Interestingly, when cyclooctatetraene (**13***) was formed from cubane (**1**), very small amounts of semibullvalene (**10**) were detected.[45] It was difficult in that case, however, to distinguish between thermal and chemically activated sources, since temperatures are high enough to convert **10** to **13** fairly rapidly.

B. Photochemistry

Our knowledge of the photochemistry of $(CH)_8$ hydrocarbons is still at a fairly primitive stage. Thus while a good deal of information is available on photoproducts, very little is known about the excited states involved, quantum yields, and pressure or wavelength dependences. A lot of early work was carried out in solution using broad-band mercury arc sources. Much of the available information was reviewed by Scott and Jones[7] in 1972, who noted many similarities between pyrolysis and photolysis products. This has led to the idea that, at least in direct (as opposed to sensitized) photolyses, vibrationally excited ground-state molecules may be responsible for much of the observed behavior.[91] There are, however, notable examples of different products in some sensitized photolyses,[92,93] leading to suggestions of triplet-state involvement. Orbital symmetry arguments have been used also with considerable effect, notably by Zimmerman's group, to explain observed patterns of behavior. While the emphasis in this review is on more recent work, earlier studies are discussed where necessary. For interpretational purposes we can take advantage of the energy surfaces (Figures 2–5) that have become available largely as a result of thermal studies (see previous section). Once again, as with thermal rearrangements, cyclooctatetraene (**13**) is a ubiquitous product.

The direct photolysis of tetracyclo[3.3.0.$0^{2,4}$.$0^{3,6}$]oct-7-ene (**4**) in solution (254 nm, room temperature)[94] leads to **13** and benzene (presumably with accompanying acetylene). D-Labeling studies show that benzene formation involves partial but by no means complete scrambling of deuterium. The suggested mechanism is shown in Scheme 18.

The partial reversibility of the conversion of **12** and **13** explains the isotopic labeling result, although it could arise through secondary photolysis of **13**. Another intermediate, not considered by the authors, that would explain this result is tetracyclo[4.2.0.$0^{2,8}$.$0^{5,7}$]oct-3-ene (**14**).

SCHEME 19

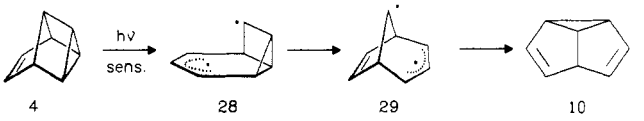

SCHEME 20

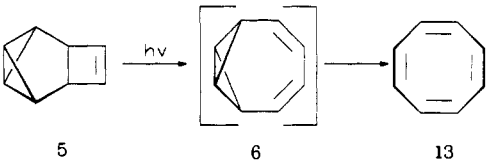

SCHEME 21

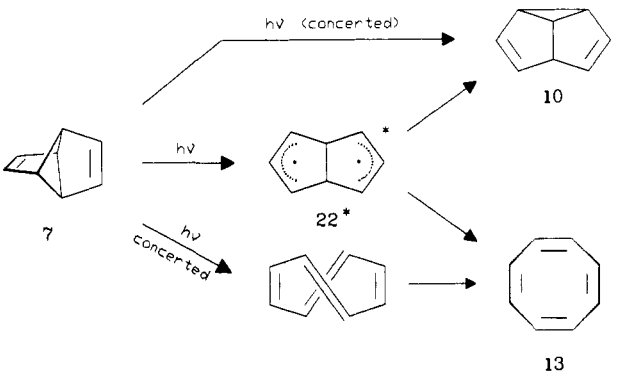

The acetone-sensitized photolysis of **4** in solution (300 nm, room temperature)[94] as well as producing **13** and benzene forms in addition some semibullvalene (**10**). This is explained by the mechanism in Scheme 19, which accounts for the observed pattern of D-labeling in **10** when starting from specifically labeled 4-*d*. This mechanism is an example of the di-π-methane rearrangement,[95] in which the triplet-state biradical **28**, prevented by reason of spin conservation from forming **12** directly, rearranges to biradical **29**, which survives long enough to permit intersystem crossing and collapse to **10**.

The solution photolysis of **5** has been only briefly studied.[50] Full mercury arc photolysis through quartz yielded cyclooctatetraene (**13**). Irradiation through Pyrex yielded no useful results. The mechanism of Scheme 20 is suspected, but trapping experiments failed to provide evidence for **6**.

Because of the facile thermal rearrangement of tricyclo[3.3.0.$0^{2,6}$]octa-3,7-diene (**7**) to semibullvalene (**10**), photochemical experiments have to be carried out at −60 °C. At this temperature, Meinwald and Tsuruta[95a] photolyzed **7** in various solutions (full Hg arc, Vycor filter) to give **13** and **10** in an approximate 2:1 ratio after correction for impurity **10** present in the reactant mixture. Blank experiments showed no conversion of **10** to **13** under the conditions of the experiments. Purely photochemical pathways for these rearrangements would be (i) for formation of **10** a concerted suprafacial [1,3]-sigmatropic shift and (ii) for formation of **13** a retro-[π2s + π2s] process giving *cis,trans,cis,trans*-cyclooctatetraene, which, if it can exist at all, is likely to revert very rapidly to **13**. An alternative mechanism involves the intermediacy of the bicyclo[3.3.0]octa-2,6-diene-4,8-diyl biradical (**22**), which, if formed, must be sufficiently excited to surmount the

SCHEME 22

SCHEME 23

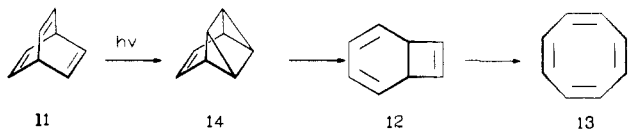

substantial barrier (ca. 20 kcal·mol^{-1}) to formation of **13** compared with that (<10 kcal·mol^{-1}) for formation of **10** (see Figure 2). These are summarized in Scheme 21. The correct mechanism is not known.

Despite the close proximity of the π bonds in *syn*-tricyclo[4.2.0.0^{2,5}]octa-3,7-diene (**9**), attempts to effect the [2s + 2s] ring-closure reaction to cubane (**1**) have not been successful. **9** is essentially inert under photochemical conditions. This has been attributed to the mixing effect of high-lying σ orbitals with the π orbitals, which would be potentially involved in the reaction. Other possible factors could be the high strain energy of **1** and the through-space bond separation.[96] The [2s + 2s] ring closure of a semibullvalene to a cuneane has been achieved for the octamethyl derivative.[74] Although it has not been reported in the unsubstituted case, we have recently obtained evidence for the photochemical production of **3** from **10**.[82,97] In solution the only reported product of semibullvalene (**10**) photolysis[64,92] (full arc, quartz tube, acetone solution, room temperature) is cyclooctatetraene (**13**). A similar result was obtained in the 1,3,5,7-tetramethyl-substituted case.[73]

The direct photolysis of barrelene (**11**) (full arc, quartz tube, methylcyclohexane solution, room temperature) gives only cyclooctatetraene (**13**).[92] The acetone-sensitized photolysis leads to semibullvalene (**10**) as well as **13**, with the ratio **10**/**13** ca. 18. This experiment of Zimmerman et al.[92] was the discovery of semibullvalene (**10**) (the remarkable thermal behavior of which is discussed in the previous section). The mechanism of this rearrangement, which was elucidated by deuterium-labeling studies represents a classic example of the di-π-methane rearrangement[95] as shown in Scheme 22.

Independent synthesis of biradical **25** via sensitized photolysis of an azo precursor[93] shows that in the triplet state **25** proceeds uniquely to **10**. The triplet of **25** cannot revert directly to **11** nor can it ring close to give **14** and therefore biradical **29** is formed, which can live long enough to spin invert and give **10**. Energy surface calculations support this description. The same biradical **29** is implicated in the photolysis of **4**, already discussed. The direct photolysis of barrelene (Scheme 23) probably involves [2s + 2s] cycloaddition to give tetracyclo[4.2.0.0^{2,8}.0^{5,7}]oct-3-ene (**14**), which thermally rearranges to **13** via **12** (see Figure 3).

Bicyclo[4.2.0]octa-2,4,7-triene (**12**), a potential intermediate in several $(CH)_8$ photochemical systems, is thermally unstable (see previous section) and therefore has to be studied at low temperatures. Photolysis at −65 °C (full arc, Vycor filter, solution with acetone sensitizer) gives only benzene and acetylene[73] (no semibullvalene (**10**) or cyclooctatetraene (**13**)). This is formally a [2s + 2s] cycloreversion, but no information

SCHEME 24

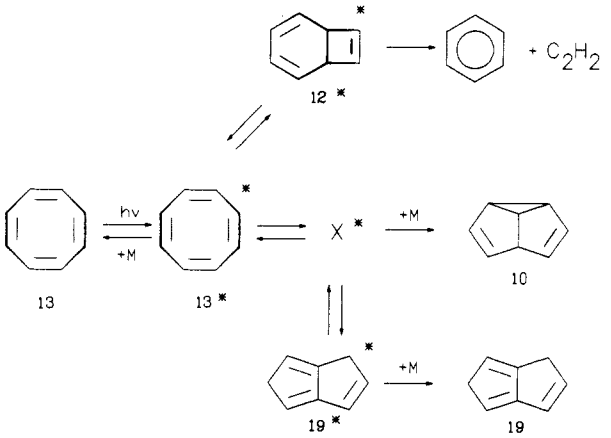

exists as to whether singlet or triplet states are involved or whether the reaction is concerted. The nonobservation of **13**, however, argues against the involvement of a vibrationally excited ground state from which formation of **13** should be overwhelmingly favored.

As with its thermal chemistry, cyclooctatetraene (**13**) offers a potentially rich photochemistry. Early work identified benzene, acetylene, and styrene as products in the gas phase, in solution, and also in a frozen matrix.[7] Solution photolysis[73] (both sensitized and direct, Vycor filter) gives in addition semibullvalene (**10**). At 185 nm, 4 and 1,3,5-octatrien-7-yne were detected.[98] Recent gas-phase studies by Dudek et al.[91] (247–312 nm) yield also 1,5-dihydropentalene (**19**) while in our own work (285–336 nm) we find additionally other dihydropentalenes, **18** and **21**, and also cuneane (**3**).[82,97]

The study by Dudek et al.[91] is the most comprehensive so far, reporting both steady-state and flash photolysis measurements. In the steady-state photolysis at 264 nm, the pressure dependence of cyclooctatetraene (**13**) disappearance suggests a zero-pressure quantum yield, Φ_{13}, close to unity. Increasing pressure reduces Φ_{13}, which leads the authors to propose a vibrationally excited **13** as the key product-forming intermediate. Further measurements of pressure dependences of product ratios suggest (i) a constant ratio of benzene to C_8H_8 isomers and (ii) a pressure-dependent ratio [**10**]/[**19**], with **10** increasing with pressure at the expense of **19**. These results are interpreted by the mechanism of Scheme 24.

This interpretation is backed up by RRKM calculations of $k(E)$ for **13*** at the several wavelengths used, which match experimental values obtained from Stern–Volmer quenching plots (with reasonably assumed collision numbers and efficiencies) and also agree with the flash photolysis results. The nature of X is discussed and the authors suggest biradical **22** as an attractive possibility. It is reasonably argued[91] that in condensed phases at sufficiently low temperatures **12** should be stabilized, so that its thermal reversion to **13** is prevented. This is as observed previously.[7,99,100] It is also argued that **10** will be stabilized in solution, as observed,[73] because of pressure quenching of X*. Pressure quenching at high temperatures in the gas phase and at long wavelengths ($\lambda > 300$ nm) has been exploited to provide a practical synthesis of semibullvalene (**10**).[101] The mechanism of Scheme 24 is further backed by photochemical studies of 1,5-dihydropentalene (**19**).[91]

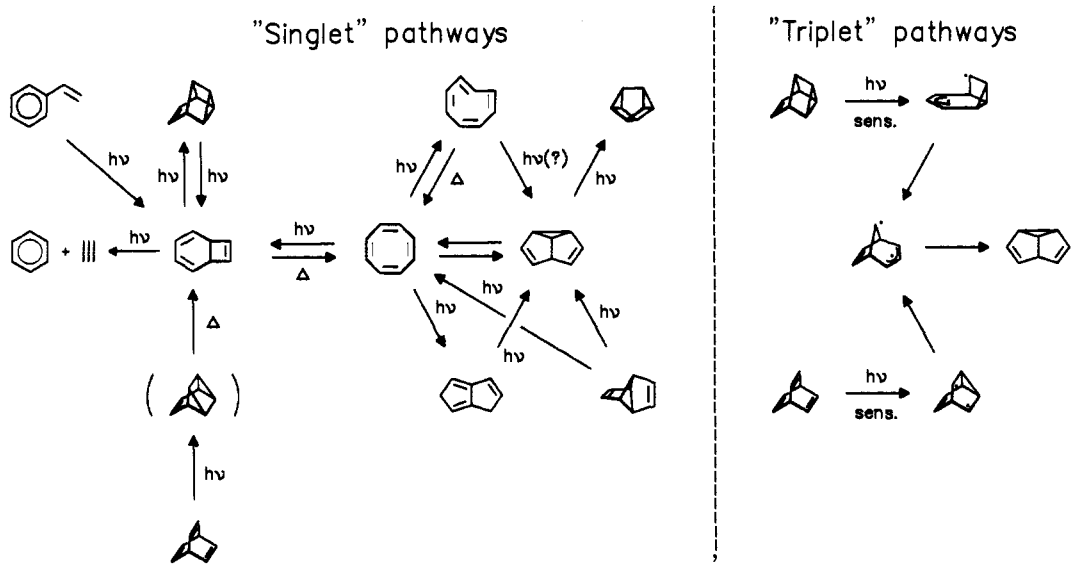

Figure 6. Observed photochemical processes for $(CH)_8$ hydrocarbons. See text for details.

SCHEME 25

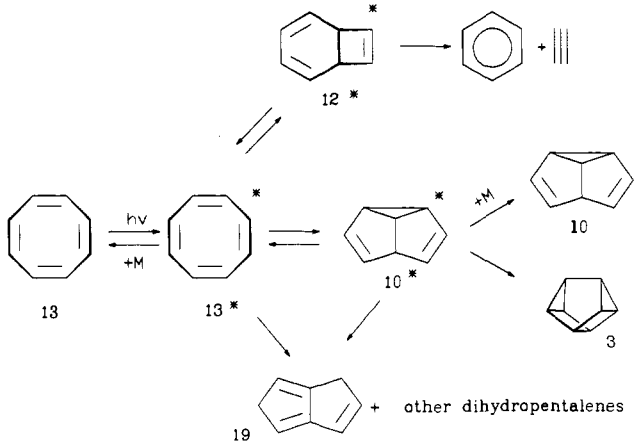

This mechanism offers an answer to the question posed by Scott and Jones:[7] How is it that the products of photolysis so closely match those of pyrolysis? The answer offered by Dudek et al.[91] is because vibrationally excited ground-state species are the key intermediates. Our own studies,[97] partially published,[82] offer a similar answer, although the results differ in some respects. The main difference, arising from the use of gas chromatography rather than UV absorption for product analysis, is that we find pressure quenching of benzene formation, so that at high pressures, semibullvalene (**10**) becomes the completely dominant product at the expense of *all* the others. This leads us to Scheme 25.

This mechanism is completely consistent with the energy surface of Figure 5. At the photon energies, at low pressures, energized cyclooctatetraene (**13**), in steady state with both **10*** and **12***, can surmount barriers leading to benzene and acetylene, dihydropentalenes **18**, **19**, and **21**, and cuneane (**3**). As pressure increases and partial collisional quenching occurs, only the lower barriers can be traversed, namely those to **10*** and **12***, which are themselves quenched. Semibullvalene (**10**) is, of course, stable, but bicyclo[4.2.0]-octa-2,4,7-triene (**12**) reverts thermally (at room temperature) to cyclooctatetraene (**13**). This mechanism, although satisfactory, still leaves open the possibility of other contributing pathways. It seems likely that vibrationally excited ground states will be largely quenched in solution. In agreement with this, quantum yields are found to be low in solution.[98] Zimmerman et al.[73] propose a triplet contribution to formation of **10** and also the possible involvement of a *trans,cis,-cis,cis*-cyclooctatetraene intermediate.[73,102] At 185 and 254 nm in solution, although the main product is benzene, 4 is also formed, possibly via the intermediacy of **12**. However, temperature dependences of product yields differ at the two wavelengths, suggesting a more complex explanation. Photolysis of **13** in a molecular beam at 193 nm produces benzene and acetylene with the release of 12% of the available energy as kinetic.[103] The authors suggest that internal conversion precedes dissociation, with the rate limited by the former. Further interpretation of this result is hampered by lack of knowledge of other products and pathways at this wavelength. A similar study of styrene photochemistry was also carried out,[103] which also implicated the formation of **12** as an intermediate prior to dissociation to benzene and acetylene.

SCHEME 26

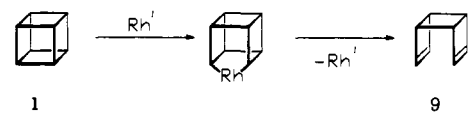

A summary of observed photochemical processes for $(CH)_8$ molecules that attempts to distinguish between singlet (which includes ground-state vibrationally excited) and triplet pathways is shown in Figure 6.

C. Catalytic Behavior

Transition-metal compounds are powerful catalysts for several valence isomerizations of strained members of the $(CH)_8$ family. In the presence of catalytic amounts of rhodium(I) complexes, cubane (**1**) isomerizes to *syn*-tricyclooctadiene (**9**). Kinetic measurements at 40 °C using NMR to follow the reactions yielded a mixed second-order rate law (first order in [catalyst] and in [1]). The most likely mechanism for the valence isomerization is via the nonconcerted oxidative addition[104] shown in Scheme 26.

By contrast, Ag(I) or Pd(II) catalytically convert cubane (**1**) quantitatively into cuneane (**3**).[105] The mechanistic route for Ag(I) is probably electrophilic.

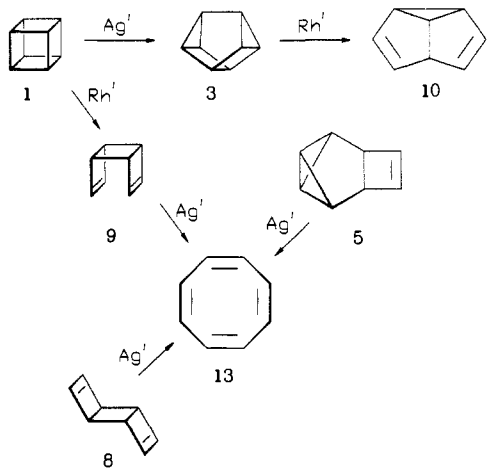

Figure 7. Catalyzed rearrangements of $(CH)_8$ hydrocarbons.

SCHEME 27

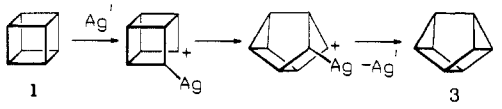

The isomerization is then the consequence of attack of Ag(I) on one of the strained bonds followed by rearrangement of the cage carbenium ion[106] (Scheme 27).

Cuneane (**3**) is isomerized to semibullvalene (**10**) by Rh(I) in an analogous manner to the **1** → **9** rearrangement.[105] Tetracyclooctene **5** is converted to cyclooctatetraene (**13**) by Ag(I), whereas other transition metals produced no useful products (in some cases no reaction).[50] *anti*-Tricyclooctadiene (**8**) is also converted to cyclooctatetraene (**13**) in the presence of silver fluoroborate with a half-life of 5 min at 56 °C.[107] These catalyzed rearrangements are summarized in Figure 7.

III. Electronic and Spectroscopic Properties of $(CH)_8$ Hydrocarbons

A. Ultraviolet Photoelectron Spectroscopy (UPES)

The interaction of nonconjugated π-electron systems has attracted great theoretical and experimental interest. Hoffmann[108] introduced the concepts of "through-space" and "through-bond" interaction between pairs of semilocalized orbitals Φ_a and Φ_b. A direct measure of this interaction is the difference in the ionization energies of the interacting orbitals Φ_a and Φ_b relative to the ionization energies of a proper reference molecule that contains isolated, noninteracting orbitals of the type Φ_a and Φ_b.[109] It is obvious that all $(CH)_8$ molecules **1**–**13** shown in Figure 1 should display interesting UPE spectra, the characteristic features of which arise from a subtle interplay of the aforementioned intramolecular interactions.

1. Cubane (1)

Cubane (**1**), in comparison with its isomer cuneane (**3**), offers an interesting example of a highly strained compound that is not as easily oxidized as its counterpart (**3**) notwithstanding the fact that **1** possesses the higher ground-state energy.[110–112] Since the electron is removed from the highest occupied molecular orbital (HOMO), it is necessary to determine both the energy and the shape of the valence orbitals of **1** and **3**.

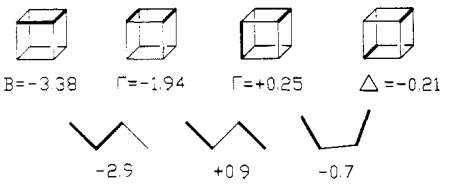

Figure 8. Cross-terms between localized STO-3G orbitals of cubane (**1**).[115] For comparison the values for simple hydrocarbons are also given. These matrix elements (in eV) have been obtained from an STO-3G model.

TABLE 2. Ionization and Orbital Energies (eV) of Cubane (1)

orbital	I_j^{m} [115]	I_j[114]	$-\epsilon_j^{MINDO/3}$ [115]	SCF[116]	SCF–Xα[117]
$3t_{2g}$	9.0–9.1	8.74	9.21	9.74	10.2
	9.5–9.6				
$1t_{2u}$	9.8–9.9		9.57	9.74	10.8
$1e_g$	13.7_5	13.62	14.36	14.74	14.9
$3t_{1u}$	14.2–14.3		13.25	15.41	15.4
$2a_{2u}$	15.6_0–15.6_5	15.34	15.89	17.30	16.5
$3a_{1g}$	17.6	(16.87)	17.44	19.11	18.5
$2t_{2g}$	18.5	(17.26)	20.00	20.56	19.9
$2t_{1u}$	22.1		28.71	25.86	22.7

The UPE spectrum of cubane (**1**) was first recorded by using a retarding-potential grid-type spectrometer.[113,114] Later high-resolution He(Iα) and He(IIα) PE spectra of cubane were measured.[115] The high symmetry (O_h) and strain of this molecule have remarkable consequences for the arrangement of the highest occupied molecular orbitals and therefore for the PE bands in the spectrum. The positions of the band maxima (I_j^m) are collected in Table 2.

Ionization energies were computed both by using Koopmans' theorem and by performing SCF calculations on the positive ion states (ΔSCF). They are included in Table 2. The 28 occupied molecular orbitals of cubane span the following irreducible representations of the group (O_h):

$$\Gamma = 3A_{1g} + 2A_{2u} + 1E_g + 3T_{1u} + 3T_{2g} + 1T_{2u} \quad (17)$$

The spectrum shows a first band system in the range 8.5–10.5 eV. Since the two radical cation states $^2T_{2g}$ and $^2T_{2u}$ are involved, the resulting Jahn–Teller instability leads to complicated band envelopes. The three maxima at 9.1, 9.55, and 9.9 eV cannot therefore be assigned to these two states in a simple way.

The second band system from 13.5 to 15.0 eV is again composed of two states, ^2E_g and $^2T_{1u}$. The vibrational fine structure of the first component of this composite band is remarkable. At 15.5 eV the spectrum displays a fine-structured band that is due to the fifth state, $^2A_{2u}$.

A convenient interpretation of the electronic structure is obtained by localization procedures.[115,117] The influence of strain on the sequence of the molecular orbitals becomes evident if the particular role of the cross-terms between localized STO-3G orbitals is investigated. These cross-terms are displayed in Figure 8. The most important feature of the cubane system is the B interaction term, which increases in absolute size with decreasing bond angle, and especially the very large 1,3-interaction matrix element $\Gamma = -1.94$ eV. The dramatic influence of this 1,3-interaction can be noticed if it is introduced as a perturbation. This is shown in Figure 9. The surprisingly large gap between the t_{2g}/t_{2u} levels on the one hand and the e_g/t_{1u} levels on the other hand is satisfactorily accounted for by this EBO model.

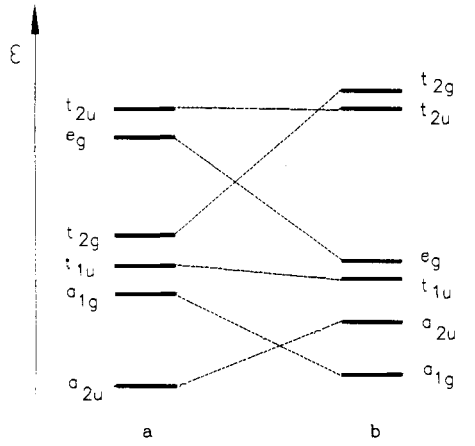

Figure 9. An equivalent bond orbital (EBO) model of cubane showing the sequence of the molecular orbitals (a) without Γ terms and (b) with inclusion of Γ matrix elements.[115]

TABLE 3. Ionization Energies from Electron Impact Studies[118]

compd	I_1, eV
styrene	8.46 ± 0.10
cyclooctatetraene (13)	8.06 ± 0.10
barrelene (11)	7.95 ± 0.10
cubane (1)	8.64 ± 0.10
anti-diene (8)	8.27 ± 0.10
syn-diene (9)	8.20 ± 0.10

TABLE 4. Ionization and Orbital Energies ($-\epsilon_i$/eV) of Octabisvalene (2)[119]

I_j^m	MINDO/3	MNDO	HAM/3	STO-3G
8.42	8.08, a_g	9.77, a_g	9.11, a_g	7.40, a_g
9.50–10.50	8.75, a_u	10.35, a_u	9.68, b_{2g}	8.38, a_u
	9.07, b_{2g}	10.80, b_{2g}	9.76, a_u	9.12, b_{2g}
	9.70, b_{1u}	10.90, b_{1u}	10.40, b_{1u}	9.64, b_{1u}
11.50–12.10	10.45, b_{3g}	12.26, b_{3g}	11.55, b_{1g}	11.45, b_{1g}
	11.40, b_{1g}	12.33, b_{1g}	11.67, b_{3g}	11.48, b_{3g}
	11.57, b_{3u}	12.65, b_{3u}	11.72, b_{3u}	12.32, b_{3u}

Since oxidation of hydrocarbons involves an electron removal from the highest occupied molecular orbital (HOMO), there is a relationship between the half-wave oxidation potential and the HOMO energy. The correlation eq 18 was found by using nine strained polycyclic hydrocarbons.[111] According to this equation, the first adiabatic ionization energy of cubane ($I_{a,1} \approx 8.46$ eV) correlates with the oxidation potential $E_{1/2} = 1.73$ V (SCE). From earlier measurements the mass spectra, appearance potential data, and ionization energies have been obtained and are given in Table 3.[118]

$$I_{a,1} = 1.28E_{1/2} + 6.25 \qquad (18)$$

2. Octabisvalene (2)

The UPE spectrum of **2** (pentacyclo-[5.1.0.0^{2,4}.0^{3,5}.0^{6,8}]octane) exhibits six distinct bands in the low-energy region; three of them are listed in Table 4 together with the results of SCF calculations.[119]

The detailed analysis of the UPE spectrum of bicyclobutane (**30**) is extraordinarily helpful in this context.[120] It is to be expected that the valence orbitals of octabisvalene represent certain symmetry-adapted combinations of the four topmost molecular orbitals of bicyclobutane (**30**). Since the energy levels of the latter are strongly dependent on the dihedral angle θ, it is not easy to assess which basis orbital energy has to be taken before combining the fragment orbitals. Moreover, the inductive perturbation of one bicyclobutane moiety on the other one is completely unknown. With this in mind, the correlation diagram in Figure 10 cannot be given more than a qualitative meaning at the moment. On the other hand, the level sequence obtained in this manner is in accordance with calculations carried out by means of some more sophisticated models (cf. Table 4).

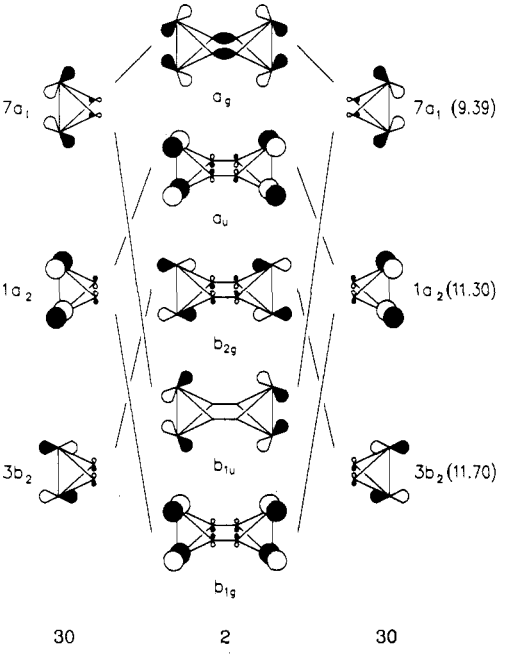

Figure 10. Qualitative correlation diagram showing the effect of combining the valence orbitals of the bicyclobutane fragments. The latter have been taken from ref 120.

TABLE 5. Ionization Energies (Maxima) I_j^m (eV) of Cuneane (3) and Assignment ($-\epsilon_i$/eV) according to Model Calculations with MM2-Optimized Geometry[121]

I_j^m	HAM/3	STO-3G
9.09	9.31, a_1	7.98, a_1
9.45	9.87, a_2	8.84, a_2
10.02	10.16, b_2	8.85, b_2
10.63	11.19, b_1	10.48, b_1
11.11	11.42, a_2	10.57, a_2
11.61	11.76, a_1	11.31, a_1
13.27	13.22, b_2	13.66, b_2

3. Cuneane (3)

Cuneane (**3**) along with cubane (**1**) is one of the most highly strained $(CH)_8$ hydrocarbons. The PE spectroscopic investigations reported recently[121] were stimulated by the following observation: In spite of the higher ground state and strain energy for cubane, cuneane is more easily oxidized than cubane. The oxidation potential of cuneane is lower than that for cubane by 0.2 V, and the adiabatic ionization energy is lower by ca. 0.25 eV.[111,112] It was therefore of interest to determine the vertical ionization energy of cuneane and to compare it with the complicated band envelope of the first PE band of cubane. Furthermore, information was desired on the nature of the orbital from which the electron comes during oxidation of **3**. Table 5 shows the ionization energies (band maxima).

From Tables 2 and 5 the following conclusions can be drawn:

(a) Lowering the symmetry from O_h (**1**) to C_{2v} (**3**) causes the levels t_{2g} and t_{2u} to split. For **3** they are now

SCHEME 28

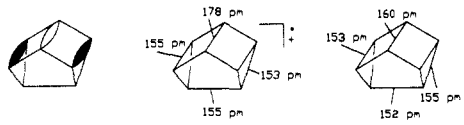

31 32 33

SCHEME 29

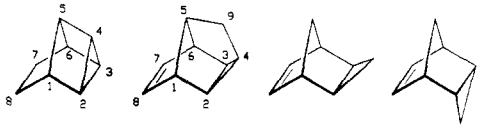

34 35 36 37

SCHEME 30

found between 9 and 12 eV.

(b) The characteristic gap between 11 and 13.5 eV in the PE spectrum of cubane (1) is also qualitatively present in the spectrum of cuneane (3). However, this gap is squeezed into the region 12–13 eV.

(c) The central σ bond in 3 may interact vicinally with the other two four-membered-ring bonds. This σ,σ interaction in four-membered rings is considerable, amounting to ca. −2.0 eV (cf. the Γ term in Figure 8).[115] Thus, the antibonding combination 31 (Scheme 28) is to be expected below the six levels that are observed in the range 9–12 eV. The HAM/3 method[122] predicts that this vicinal antibonding σ orbital 31 is the HOMO for 3.

(d) The complex band envelope of the first PE band of cubane (1) makes it difficult to locate the ionization energy that leads to the symmetrical cubane cation radical. One possibility is that the second maximum at 9.6 eV (the centroid of the band system) is to be interpreted as the central maximum of the cubane $^2T_{2g}$ state. If this is correct the first vertical ionization energy of cuneane (3) would be lower than that of cubane, and it would then run parallel to the lower adiabatic ionization energy of cuneane. The structure of the adiabatic radical cation 32 of 3 in its electronic ground state was calculated by using an open-shell MINDO/3 method.[121] The bond length changes show that the most pronounced effect is observed for the central bond. The increase from 160 pm (neutral ground state 33 of 3) to 178 pm in 32 agrees with the fact that the photoelectron is removed from an orbital that is significantly localized in the central bond (cf. 31).

4. *Tetracyclo[3.3.0.0^{2,4}.0^{3,6}]oct-7-ene (4)*

In view of the large amount of strain energy present in 4, a study of its molecular orbital structure was of interest.[123] Since the position and the splitting of the highest occupied levels of the cyclopropane ring, e_s and e_a, are of special interest, a series of the related compounds 34–37 (Scheme 29) is discussed as well.

The experimental and calculated (Hartree–Fock–Slater method) ionization energies are summarized in Table 6.

The discussion is based on semilocalized orbitals, i.e., the π orbital of the double bond and the Walsh orbitals

TABLE 6. Experimental (I_j^m/eV) and Calculated (HFS) Ionization Energies of 4, 34, and 35[123]

compd	I_j^m	HFS	molecular orbital
4	8.95	8.0	13a′, π(C=C)
	9.15	8.1	7a″, 60% $e_a(C_2C_3C_4)$ − 30% "e_a"$(C_1C_5C_6)$
	9.90	8.8	12a′, $e_s(C_2C_3C_4)$
	10.95	9.9	6a″, mainly $(C_1C_5C_6)$
	11.25	10.1	11a′, C_4C_5 bridge
34	8.85	7.6	8a″, 65% $e_a(C_2C_3C_4)$ − 20% "e_a"$(C_1C_5C_6)$
	9.70	8.4	13a′, $e_s(C_2C_3C_4)$
	9.70	8.4	7a″, mainly $(C_1C_5C_6)$
35	8.75	7.3	15a′, π(C=C)
	9.50	7.7	8a″, $e_a(C_2C_3C_4)$
	9.65	8.1	14a′, $e_s(C_2C_3C_4)$

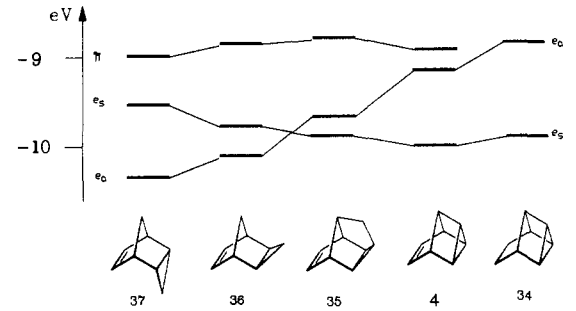

Figure 11. Experimental orbital correlation diagram ($\epsilon_i = I_i^m$) for 4 and 34–37. The reversal in the e_s,e_a sequence for 4 and 34 is clearly demonstrated. The nearly degenerate e_s and e_a levels in 35 correspond to the usual situation in 1,2,3-trialkylated cyclopropanes.[123,124]

SCHEME 31

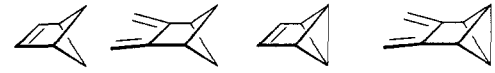

38 39 40 41

of the cyclopropyl moiety (Scheme 30). The Walsh orbitals may be written as

$$e_s = (1/2^{1/2})(p_2 - p_3) \quad (19a)$$

$$e_a = (1/6^{1/2})(2p_1 - p_2 - p_3) \quad (19b)$$

It has been shown that the orbital sequence in 36 and 37 is $\pi > e_s > e_a$, the splitting e_s–e_a amounting to 0.6 eV in 36 and to 0.8 eV in 37.[124] The reason for the lower ionization energy of e_s in 36 and 37 is comprehensible. Since the shift in $\epsilon(e_a)$ and $\epsilon(e_s)$ (induced by an alkyl substituent in position μ of the cyclopropane ring) is proportional to the squared coefficient of the atomic orbital p_μ in eq 19, the linear combination e_s in 36 and 37 is destabilized more strongly than the antisymmetric orbital e_a. Compounds 4 and 34, however, are found to be unique in having e_a well above e_s.[123] On the other hand, compound 35 displays nearly degenerate e_a and e_s levels. Obviously, the unusual behavior of 4 and 34 is related to the particular cage structure of these molecules. The theoretical analysis shows that the direct neighborhood of C-4 and C-5 in 4 and 34 is responsible for a strong destabilization of e_a. The e_a orbital has a large amplitude at C-4. When this atom is brought close to C-5 to form the C-4/C-5 bridge, an antibonding interaction with a fragment orbital C-1/C-5/C-6 of equal symmetry pushes the e_a combination upward. The correlation diagram for these molecules is shown in Figure 11.

TABLE 7. Experimental Vertical Ionization Energies I_j^m (eV) and Calculated Orbital Energies ϵ_j (eV) of Octavalene (6)[126]

I_j^m	character	ZDO	MNDO	STO-3G
8.09 vib	$2a_2$, $\pi-\sigma$	7.9	8.82	6.23
8.28				
9.25	$9a_1$, σ	9.3	10.18	8.22
10.25	$3b_2$, $\pi-\sigma$	10.3	10.74	9.31
11.72	$1a_2$, $\sigma+\pi$	11.9	12.27	11.46
12.20	$2b_2$, $\sigma+\pi$	12.0	12.49	12.01

5. Octavalene (6)

With data from UPE spectroscopic investigations of **38**, **39**, **40**, and **41**, (Scheme 31), it has been shown that there is a stronger interaction between a π fragment and the bicyclobutane moiety compared to the cyclobutane fragment.[125] The resonance integral β derived from the spectra amounts to $\beta = -1.9$ eV for **38** and **39** and to $\beta = -2.3$ eV for **40** and **41**.

The $(CH)_8$ hydrocarbon **6** (octavalene) represents a nice example to check these interaction parameters. The ionization energies of **6** and the results of simple ZDO and more sophisticated calculations are given in Table 7.[126]

The description of the electronic structure of **6** in terms of fragment molecular orbitals is an adequate and clear analytical procedure. The wave functions for the two fragments of **6** are the π molecular orbitals of butadiene and the valence orbitals of bicyclobutane, the latter being displayed in Figure 10. The wave functions are given in eq 20a–e.

$$\pi_1(b_2) = 0.37(p_a + p_d) + 0.60(p_b + p_c) \quad (20a)$$

$$\pi_2(a_2) = 0.60(p_a - p_d) + 0.37(p_b - p_c) \quad (20b)$$

$$\psi_1(a_2) = -0.5(p_h - p_e - p_f + p_g) \quad (20c)$$

$$\psi_2(b_2) = 0.5(\Phi_h - p_e - \Phi_g - p_g) \quad (20d)$$

$$\psi_3(a_1) = (1/2^{1/2})(\Phi_f - \Phi_h) \quad (20e)$$

In (20) the p's are p_π atomic orbitals, while the Φ's are hybrid atomic orbitals. With appropriate basis orbital energies and the interaction parameter $\beta = -2.3$ eV as resonance integral between the butadiene and the bicyclobutane fragments, the orbital sequence of Figure 12 is obtained for the five topmost valence orbitals in octavalene (**6**).

This study confirms the assumption of a stronger interaction of an olefinic moiety with the bicyclobutane fragment than with a cyclobutane ring.

6. Tricyclo[3.3.0.0^{2,6}]octa-3,7-diene (7)

No experimental UPE studies have as yet been reported. However, diene **7** has been investigated theoretically by means of CNDO/1, MINDO/3, and ab initio (STO-3G) calculations.[127-129] The most remarkable result of these studies is the observation that the central cyclobutane ring in **7** acts as a *relay* fragment, i.e., a structural unit possessing orbitals that enforce the interaction between remote π orbitals.

The two occupied π orbitals of **7** combine to a degenerate pair of molecular orbitals that interact with the σ frame. The unoccupied π^* orbitals yield linear combinations of a_2 and b_1 symmetry. The split between these orbitals amounts to 1.06 eV, $\Phi(b_1)$ lying above $\Phi(a_2)$. Experimental evidence obtained so far relates

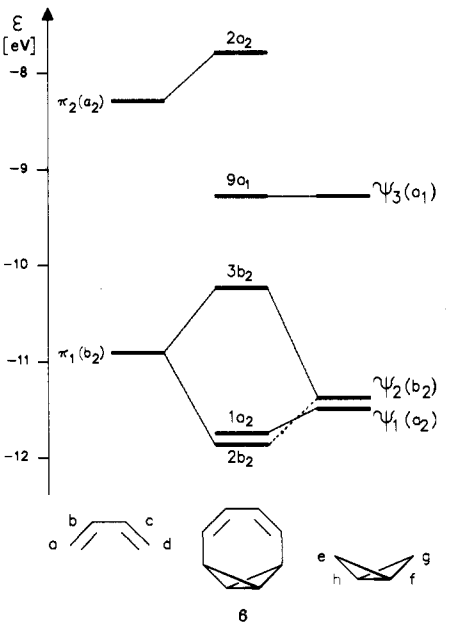

Figure 12. Fragment orbital analysis of octavalene (**6**). The fragment orbitals of bicyclobutane are the same as in Figure 10.[126]

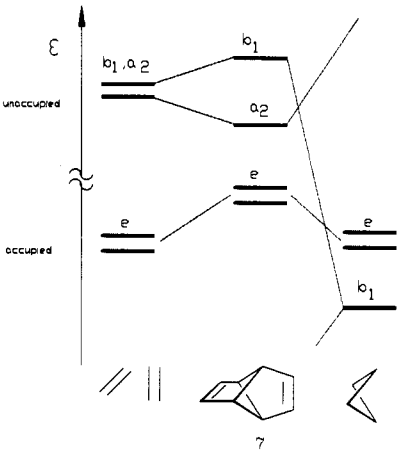

Figure 13. Qualitative interaction diagram showing the effect of the relay fragment cyclobutane in the hydrocarbon **7**.[128]

to the low energy of the first transition at 300 nm. A qualitative interaction diagram is shown in Figure 13.

7. anti- and syn-Tricyclo[4.2.0.0^{2,5}]octa-3,7-diene (8 and 9)

Among the $(CH)_8$ hydrocarbons dienes **7**, **8**, and **9** are of special interest because transannular π,π interactions are possible using symmetry-adapted Walsh orbitals of the central cyclobutane as transmitter and *relay* orbitals. Several articles deal with this phenomenon in **8** and **9**. The first such investigation reported a UPE study and interpreted the experimental data by comparison with the di- and tetrahydro derivatives within the concept of through-space and through-bond interactions.[130] The electronic structure and valence isomerization of **8** and **9** have been studied by using the semiempirical MINDO/1 and MINDO/2 models.[131] A third publication repeated the UPE measurements and gave an interpretation of the spectra that was based on MINDO/2 calculations with geometry optimization.[132] Ab initio calculations gave a sequence of high-lying π orbitals in both **8** and **9**, without interspersed σ-dominated orbitals.[133] In an article entitled "A Quantitative

TABLE 8. Experimental Ionization Energies I_j^m (eV) and Calculated Orbital Energies ϵ_j (eV) of 8 and 9

			assignment				
compd	$I_j^{m\ 130}$	$I_j^{m\ 132}$	ref 130	ref 132	ref 135	ref 137	ref 137a
8	8.96	8.90	$\pi_+(a_g)$	$\pi_+(a_g)$	$\pi_+(a_g)$	$\pi_+(a_g)$	$\pi_+(a_g)$
	9.93	9.93	$\pi_-(b_u)$	$\pi_-(b_u)$	$\sigma(b_u)$	$(\pi_- - \sigma)(b_u)$	$\pi_-/\sigma(b_u)$
	10.13	10.27	$\sigma(a_u)$	σ	$\pi_-(b_u)$	$(\sigma+\pi_-)(b_u)$	$\sigma/\pi_-(b_u)$
	10.57	10.56	$\sigma(b_u)$	$\sigma(b_g)$	$\sigma(a_u)$	$\sigma(a_u)$	$\sigma(b_g)$
9	9.08	9.08	$\pi_+(a_1)$	$\pi_+(a_1)$	$\pi_+(a_1)$	$\pi_+(a_1)$	$\pi_+(a_1)$
	9.44	9.46	$\pi_-(b_2)$	σ	$\sigma(b_2)$	$(\pi_- - \sigma)(b_2)$	$\pi_-/\sigma(b_2)$
	9.87	9.87	$\sigma(b_2)$	$\pi_-(b_2)$	$\pi_-(b_2)$	$(\sigma+\pi_-)(b_2)$	$\sigma/\pi_-(b_2)$
	10.67	10.71	$\sigma(a_2)$	$\sigma(a_1)$	$\sigma(a_2)$	$\sigma(a_2)$	$\sigma(a_2)$

TABLE 9. Experimental Ionization Energies I_j^m (eV) of 10, 38, and 39[138]

compd	I_1^m	I_2^m	I_3^m	I_4^m
10	8.5	8.8	10.4	11.4
38	8.4	8.8	10.2	11.0
39	8.3	8.7	10.4	10.9

SCHEME 32

38 39

Assessment of Through-space and Through-bond Interactions" a critical review of the results obtained so far has been given.[134] A study of cyclopropanated homo and bishomo derivatives also reinvestigated the parent compounds 8 and **9**.[135] Both the MINDO/3 procedure and a simple correlation technique predict the orbital sequence $\pi_+ > \sigma > \pi_-$, in contrast to the results of an ab initio STO-3G treatment. The situation became even more complicated when it was found that the MNDO model gave results in harmony with the original interpretation.[136] The origin of these discrepancies is the extreme sensitivity of through-space and through-bond interaction with respect to small changes in geometry.[134] Thus, it has finally been observed, using the HAM/3 model with MM1/MM2 geometries, that there is—dependent on the chosen geometry—a non-negligible, significant mixing of $\pi_-(b_u)$ and $\sigma(b_u)$ orbitals in 8 and of $\pi_-(b_2)$ and $\sigma(b_2)$ levels in **9**.[137] Recently, ab initio CI calculations, using a partially MINDO/2-optimized structure, gave results in accordance with the simple HAM/3 model.[137a]

In Table 8 the experimental ionization energies and calculated orbital energies are listed.

The interpretation of the interaction shown in Figure 14 is based on HAM/3 calculations[122,137] and on basis orbital energies that are assigned by using an empirical correlation technique.[130,135]

8. Semibullvalene (10)

In Table 9 the vertical ionization energies of semibullvalene (**10**), barbaralene (**38**), and dihydrobullvalene (**39**) are listed[138] (Scheme 32). The four highest occupied molecular orbitals are built from the two originally degenerate Walsh orbitals of cyclopropane and the two π orbitals of the double bonds. Allowing for the through-space and through-bond interaction among the π basis orbitals yields the symmetry-adapted combinations $\pi(a')$ and $\pi(a'')$. Conjugation between the Walsh orbitals e_s and e_a (cf. (19) and Scheme 30) and the π combinations leads to orbital energies for the four topmost occupied molecular orbitals of **10**, **38**, and **39**. The essential correctness of these predictions is strongly

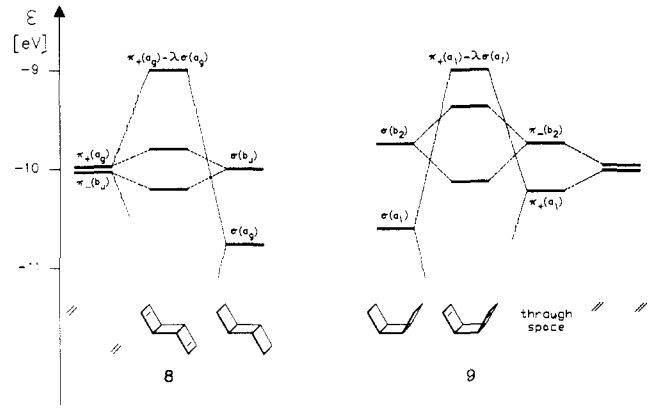

Figure 14. Correlation diagram for 8 and 9. Basis orbital energies have been assigned according to ref 130 and 135: $\epsilon_0(\pi) = -10.0$ eV, $\epsilon_0(\sigma(b_u)) = -10.0$ eV, and $\epsilon_0(\sigma(b_2)) = -9.7$ eV. Basis energies for $\sigma(b_u)$ and $\sigma(b_2)$ are clearly different. The through-space interaction amounts to 0.4–0.6 eV; the value 0.6 eV has been used in the figure. Mixing of π_- with $\sigma(b_u,b_2)$ is significant. As a function of geometry and SCF model varying combinations $(\pi_- - \lambda\sigma)$ are obtained.

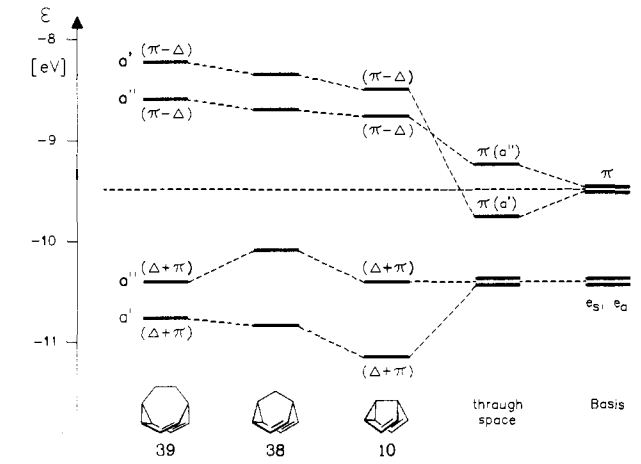

Figure 15. Correlation between the experimental ionization energies $I_j^m = -\epsilon_j$ (in eV) of **10**, **38**, and **39**. The *Walsh* character is indicated by using Δ in the combination. The broken line shows the shift of the basis orbital energy when going from **10** to **39** owing to the increasing σ system.

supported by the observed close resemblance of the UPE spectra of **10**, **38**, and **39**.[138] In Figure 15 the experimental vertical ionization energies of these hydrocarbons have been correlated. In contrast to **39**, the a'' orbital energies in **10** and **38** are no longer split symmetrically with respect to those of the interacting a'' pair. This is due to increasing tightness of the cage molecules, which will induce mixing with other σ orbitals.

The UPE spectrum of semibullvalene (**10**) has not been displayed as yet. Figure 16 therefore shows the

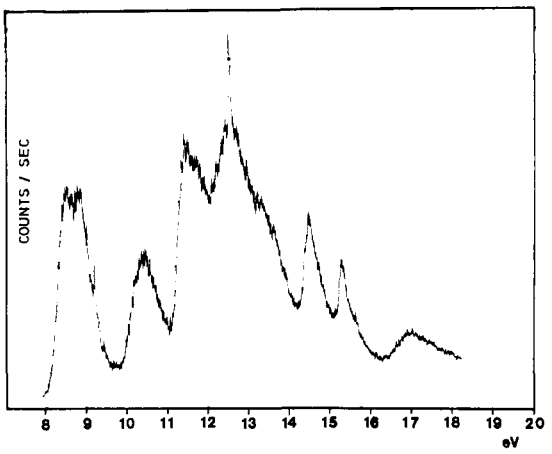

Figure 16. UPE (He(I)) spectrum of semibullvalene (10).[139]

TABLE 10. Experimental (I_j^m/eV) and Calculated Ionization Energies (eV) of Barrelene (11)[140,141] a

		MINDO/2	ab initio CI[141]	
I_j^m	I_G	(θ = 113°)	Koopmans	shake-up
8.23	8.24	9.38, $\pi(a_2')$	8.15, $\pi(a_2')$	
9.65_{JT}	9.63	9.72, $\pi(e')$	9.63, $\pi(e')$	
10.02_{JT}				
11.25	11.11	9.83, $\sigma(a_1')$	11.24, $\sigma(e'')$	
11.9_5		10.25, $\sigma(e'')$	11.95, $\sigma(a_1')$	12.24 (e'')
				12.34 (e'')
				13.54 ($a_2'e'e''$)
13.2	13.1		13.74, $\sigma(a_2'')$	13.74 ($a_2'e'e''$)
13.9			14.36, $\sigma(e')$	14.49 (e'')
				14.83 ($a_2'e'e''$)
14.7	14.5		14.72, $\sigma(e')$	

[a] I_G: Values obtained with a grid-type spectrometer.[113] θ is the angle between axial C–H and C–C single bonds. JT: Jahn–Teller.

PE band system in the range from 8 to 18 eV.[139]

9. Barrelene (11)

Table 10 shows the experimental ionization energies and the assignment according to various theoretical procedures.[140,141] With respect to the problem of the interaction of nonconjugated π orbitals barrelene (11) is obviously a key compound. The first two bands in the PE spectrum of 11 must be classified as π bands. The complex structure of the second band can be easily understood. The $^2E'$ state of the radical cation undergoes a Jahn–Teller distortion.[140] Difficulties arise when one tries to correlate the bands at higher ionization potentials with results from model calculations. The MINDO/2 procedure yields orbital energies that are dependent on the angle θ between the bridgehead C–H and the C–C single bonds. According to a more sophisticated ab initio CI calculation,[141] $\sigma(e'')$ lies above $\sigma(a_1')$ in contrast to the MINDO/2 method (cf. Table 10). The CI procedure also allows for shake-up states of the type $(1a_2')^2 \rightarrow (1a_2')^0(e'')^1$ or $(a_2')^2(e')^2 \rightarrow (a_2')^1(e')^1(e'')^1$. Barrelene has UV-absorption maxima at 239 and 208 nm.[142] Calculated values for the lowest triplet and singlet are 3.82 and 6.04 eV, respectively, both having $a_2'e''$ occupancy.[141] Thus the shake-up states, which can be envisaged as ionization of the triplet, will probably occur from 3.8 + 8.25 = 12 eV upward.[141]

The split between the first two π bands, $\epsilon(\pi(a_2')) - \epsilon(\pi(e'))$ = 1.6 eV is the resultant of two effects: through-space interaction and through-bond interaction with lower lying σ orbitals. The consequence of an increasing number of double bonds (and therefore strain) in the bicyclo[2.2.2]octane system on ionization energies can be seen in Figure 17.

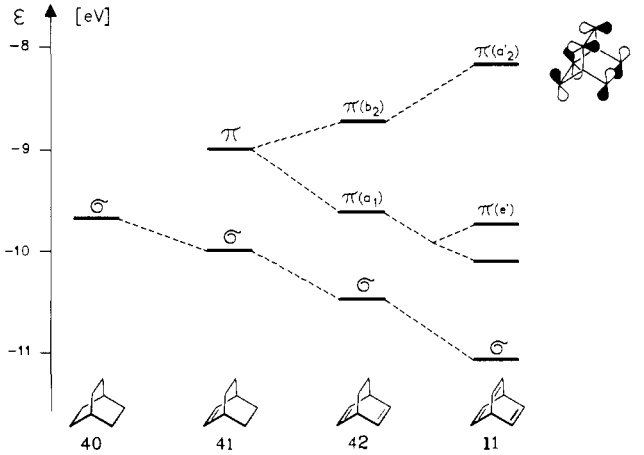

Figure 17. Correlation diagram of the ionization energies of 11, 40, 41, and 42.[140]

SCHEME 33

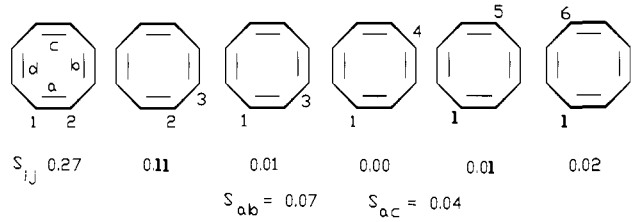

Since the interaction between any two of the basis orbitals π_i in $\pi(a_2')$ is antibonding (cf. Figure 17), removal of an electron will reduce the repulsion between all pairs of bonds. This reduced repulsion between the π bonds will lead to a deformation in which the apical methine groups move away from each other. Thus the vibrational fine structure will be dominated by the totally symmetric mode $\tilde{\nu}$ = 570 cm^{-1}.[140]

It has been concluded from STO-3G calculations that molecules like barrelene are destabilized by homoconjugation but stabilized by hyperconjugation.[36]

10. Cyclooctatetraene (13)

The UPE spectrum of cyclooctatetraene (13) has been investigated by several groups.[143,144] In 13 several interactions have to be discussed (see Scheme 33). A simple LCBO model yields for the four π orbitals (symmetry D_{2d})

$$\epsilon(\pi(5a_1)) = A - 2B_{ab} + B_{ac} \quad (21a)$$

$$\epsilon(\pi(7e)) = A - B_{ac} \quad (21b)$$

$$\epsilon(\pi(4b_2)) = A + 2B_{ab} + B_{ac} \quad (21c)$$

The experimental results can be accommodated only if A = −9.8 eV, B_{ab} = −0.7 eV, and B_{ac} = 0 eV. It is interesting that the energy gaps between bands 1 and 2, Δ_{12}, and bands 2 and 3, Δ_{23}, are virtually identical: $\Delta_{12} = \Delta_{23}$ = 1.36 eV. A most important feature is that B_{ac} (the interaction parameter between two opposite orbitals π_a and π_c) is practically zero in 13. This is a clear indication that there is a complete cancellation of through-space and through-bond interactions between the orbitals π_a and π_c.[144] Experimental ionization energies and assignments are given in Table 11.

TABLE 11. Experimental (I_j^m/eV) and Calculated Ionization Energies (eV) of Cyclooctatetraene (13)[144,145]

			ab initio[145]	
I_j^m	LCBO	ab initio[144]	Koopmans	shake-up
8.42	8.41	8.72, $\pi(5a_1)$	7.92, $\pi(5a_1)$	
9.78	9.77	10.44, $\pi(7e)$	9.52, $\pi(7e)$	
11.15	11.13	11.62, $\pi(4b_2)$	10.96, $\pi(4b_2)$	10.68, $^2A_2$
				10.88, $^2A_2$
11.55		12.61, $\sigma(3b_1)$	11.75, $\sigma(3b_1)$	11.40, ^2E
				11.99, $^2A_2$

The number of low-lying shake-up states of A_2 symmetry is notable.[145] This is due to the low-lying LUMO $\pi^*(3a_2)$. The first state of this kind corresponds to the HOMO–LUMO process $5a_1^2 \rightarrow 3a_2^1$. Another shake-up state is calculated at 11.4 eV, $(5a_1)^2(7e)^4 \rightarrow (5a_1)^1(7e)^3(3a_2)^1$.

The asymmetry parameter β of the photoelectron angular distribution has been determined for the four highest occupied orbitals.[146]

B. Electron Transmission Spectroscopy

Cyclooctatetraene (13) has been investigated.[147] The ET spectrum displays broad resonances at 1.73, 3.47, and 6.37 eV. There is no vibrational structure, nor is there evidence for excited vibrational levels of the stable ground-state anion. Presumably both the mono- and divalent anions are planar in solution and the gas phase. The vacant orbitals are $\pi^*(a_2)$, $\pi(e)$, and $\pi(b_2)$ (symmetry D_{2d}). The $^2A_2$ state is stable; thus the resonances at 1.73 and 3.47 eV are assigned to the excited states ^2E and $^2B_2$. The first vertical electron affinity ($^2A_2$) is 0.83 eV.

Cyclooctatetraene (13) was found to readily form negative ions through unimolecular nondissociative thermal electron attachment.[148]

C. Ultraviolet Spectroscopy

The long-wavelength absorption of diene 7 at 300 nm ($\epsilon \approx 190$) has been rationalized by means of CNDO/S calculations.[127]

The absorption spectrum of barrelene (11) was first measured in an ethanol solution, and maxima were reported at 239 nm ($\epsilon \approx 300$) and at 208 nm ($\epsilon \approx 1100$).[142] Absorption and magnetic circular dichroism (MCD) studies have been carried out in cyclohexane solution.[149,150] Two excited states are related to a promotion of an electron from the HOMO (a_2') to the LUMO (e''): At 296 nm (4.2 eV) $^1A_1' \rightarrow {}^3E''$ and at 240 nm (5.2 eV) $^1A_1' \rightarrow {}^1E''$. According to computations the largest oscillator strength is carried by a $^1A_1' \rightarrow {}^1A_2''$ transition around 170 nm.[150] An absorption and MCD study of barrelene in the gas phase unveiled a strong valence band at 178 nm, and this transition has been assigned to $^1A_1' \rightarrow {}^1A_2''$ in accordance with the theoretical predictions.[142]

The near-ultraviolet spectrum of cyclooctatetraene (13) can be described as a broad maximum of low intensity over the region 310–260 nm (4.00–4.77 eV) and a strong end absorption with a shoulder at 205 nm (6.05 eV).[150] Semiempirical and ab initio CI calculations were applied to the electronic transitions of 13.[145,150,151] The first excited singlet state ($^1A_2$) is computed at 4.37 eV and has the occupancy $5a_1 3a_2^*$. The higher singlet states are $5a_1 8e^*$ (5.46 eV, ^1E), $4b_2 3a_2^*$ (5.75 eV, $^1B_1$), and $5a_1^0 3a_2^{2*}$ (6.08 eV, $^1A_1$). The last case (S_4) is a doubly excited state.[145] A MCD study of 13 has been carried out.[152]

D. Miscellaneous

The influence of bicyclo[1.1.0]butane strain on the ^{13}C spectra of 5, 6, and related compounds has been studied.[153] Condensed-phase vibrational spectra are reported for cubane (1), cubane-*d*, *sym*-cubane-d_2, *sym*-cubane-d_6, and cubane-d_8.[154] Vibrational assignments have been made for all the fundamentals of all five compounds. The vapor-phase infrared spectrum of 1 has also been investigated.[155] A detailed normal coordinate analysis has been performed.[156] The equilibrium geometry and vibrational frequencies of 1 have been studied by using accurate ab initio SCF calculations.[157,158] Confirmation of the octahedral symmetry and improved bond length measurements are obtained from high-resolution tunable laser spectra of the three infrared-active fundamental vibrations of cubane (1) in the vapor phase.[159] Raman and infrared spectra of semibullvalene (10) have been recorded and 41 fundamentals have been identified.[160] Infrared spectra of gaseous, liquid, and polycrystalline barrelene (11) as well as Raman spectra for the liquid were measured.[161] The possible significance of the force constant values with regard to strain and rigidity of barrelene (11) has been discussed. A harmonic–vibration analysis for the vibrations of cyclooctatetraene (13) was performed, and the corresponding symmetry force constants have been given.[162]

IV. Structure

An X-ray structure determination of cubane (1) gave the space group $R3$ with the cell constants $a = 534.0 \pm 0.2$ pm and $\alpha = 72.26 \pm 0.05°$. There is one molecule per unit cell. The molecule has cubic symmetry with C–C bond length 154.9 ± 0.3 pm.[163] The electron diffraction data of gaseous cubane are also consistent with O_h symmetry, and the C–C bond length is much longer than in cyclobutane, r(C–C) = 157.5 (1) pm.[164] Quantum chemical as well as force-field calculations of the cubane geometry are available.[165–169] The structure of semibullvalene (10) in the gas phase was investigated by electron diffraction. The cyclopentene rings in 10 are bent, with a pucker angle of about 18°.[170] A gas electron diffraction study of barrelene (11) gave bond lengths r_g(C=C) = 133.8 (2) pm and r_g(C–C) = 154.1 (1) pm. The intramolecular strain has been analyzed with the aid of calculations based on a consistent force field.[171] The structure of cyclooctatetraene (13) has been determined both by electron diffraction and by low-temperature X-ray diffraction.[172,173] The carbon–carbon single- and double-bond distances are r_g = 147.5 pm, r_g = 134.0 pm (ED), and r = 147.0, 146.5, 147.3 pm, r = 133.3 pm (X-ray).

V. Acknowledgment

We appreciate financial support of our own work by the Deutsche Forschungsgemeinschaft, the Fonds der Chemischen Industrie, and BASF AG. We thank R. Srinivasan for private correspondence. K. Hassenrück greatfully acknowledges a fellowship from the Feodor-Lynen-Foundation.

VI. References

(1) Small and Medium Rings. Part 73. Part 72: Hake, H.; Landen, H.; Martin, H.-D.; Mayer, B.; Steigel, A.; Distefano, G.; Modelli, A. *Tetrahedron Lett.* **1988**, *50*, 6601. This is also Part 6 of "C_8H_8 Hydrocarbons". Part 5: Hassenrück, K.; Martin, H.-D.; Mayer, B. *Chem. Ber.* **1988**, *121*, 373.
(2) Liebman, J. F.; Greenberg, A. *Chem. Rev.* **1976**, *76*, 311.
(3) Balaban, A. T. *Rev. Roum. Chim.* **1966**, *11*, 1097.
(4) Tausch, M. W.; Hass, E. C.; Plath, P. J. *Match* **1979**, 289.
(5) Balaban, A. T. *Rev. Roum. Chim.* **1986**, *31*, 679.
(6) Balaban, A. T. *Rev. Roum. Chim.* **1986**, *31*, 695.
(7) Scott, L. T.; Jones, M. *Chem. Rev.* **1972**, *72*, 181.
(8) Smith, L. R. *J. Chem. Educ.* **1978**, *55*, 569.
(9) Balaban, A. T.; Bandu, M. *J. Chem. Educ.* **1984**, *61*, 766.
(10) Gajewski, J. J. *Hydrocarbon Thermal Isomerizations*; Academic Press: New York, 1981.
(11) Kybett, B. D.; Carroll, S.; Natalis, P.; Bonnell, D. W.; Margrave, J. L.; Franklin, J. L. *J. Am. Chem. Soc.* **1966**, *88*, 626.
(12) Prosen, E. J.; Johnson, W. H.; Rossini, F. D. *J. Am. Chem. Soc.* **1950**, *72*, 626.
(13) Turner, R. B.; Meador, W. R.; Doering, W. von E.; Knox, L. M.; Mayer, J. R.; Wiley, D. W. *J. Am. Chem. Soc.* **1957**, *79*, 4127.
(14) Turner, R. B. *J. Am. Chem. Soc.* **1964**, *86*, 3586.
(15) Fuchs, R.; Peacock, L. A. *J. Phys. Chem.* **1979**, *83*, 1975.
(16) Martin, H.-D.; Urbanek, T.; Braun, R.; Walsh, R. *Int. J. Chem. Kinet.* **1984**, *16*, 117.
(17) Martin, H.-D.; Urbanek, T.; Walsh, R. *J. Am. Chem. Soc.* **1985**, *107*, 5532.
(18) Squillacote, M. E.; Bergman, A. *J. Org. Chem.* **1986**, *51*, 3910.
(19) Baird, N. C. *Tetrahedron* **1970**, 2185.
(20) Iwamura, B. H.; Morio, K.; Kurui, T. L. *Chem. Commun.* **1971**, 1408.
(21) Bingham, R. C.; Dewar, M. J. S.; Lo, D. H. *J. Am. Chem. Soc.* **1975**, *97*, 1294.
(22) Dewar, M. J. S.; Zoebisch, E. J.; Healy, E. F.; Stewart, J. P. *J. Am. Chem. Soc.* **1985**, *107*, 3902.
(23) Allinger, N. L.; Tribble, M. T.; Miller, M. A.; Wertz, D. H. *J. Am. Chem. Soc.* **1971**, *93*, 1637.
(24) Engler, E. M.; Andose, J. D.; Schleyer, P. von R. *J. Am. Chem. Soc.* **1973**, *95*, 8005.
(25) Allinger, N. L. *J. Am. Chem. Soc.* **1977**, *99*, 8127.
(26) Jaime, C.; Osawa, E. *Tetrahedron* **1983**, *39*, 2769.
(27) Ivanov, P. U. *J. Chem. Res. (S)* **1985**, 86; *J. Chem. Res. (M)* **1985**, 1173.
(28) Allinger, N. L.; Yuh, Y. H. *Pure Appl. Chem.* **1983**, *55*, 191.
(29) Benson, S. W. *Thermochemical Kinetics*; Wiley: New York, 1976.
(30) Gasteiger, J.; Dammer, O. *Tetrahedron* **1978**, *34*, 2939.
(31) George, P.; Trachtman, M.; Bock, C. W.; Brett, A. W. *Tetrahedron* **1976**, *32*, 317.
(32) Disch, R. L.; Schulman, J. M.; Sabio, M. L. *J. Am. Chem. Soc.* **1985**, *107*, 1904.
(33) Ibrahim, M. R.; Schleyer, P. von R. *J. Comput. Chem.* **1985**, *6*, 157.
(34) Wiberg, K. B. *J. Comput. Chem.* **1984**, *5*, 197.
(35) Wiberg, K. B. *J. Org. Chem.* **1985**, *50*, 5285.
(36) Leroy, G.; Peeters, D.; Ruelle, J.-L. *J. Chim. Phys.* **1974**, *71*, 476.
(37) Iwamura, H.; Kihara, H. *Bull. Chem. Soc. Jpn.* **1975**, *48*, 512.
(38) Hassenrück, K.; Martin, H.-D.; Walsh, R. *Chem. Ber.* **1988**, *121*, 369.
(39) Martin, H.-D.; Pföhler, P.; Urbanek, T.; Walsh, R. *Chem. Ber.* **1983**, *116*, 1415.
(40) Martin, H.-D.; Urbanek, T.; Pföhler, P.; Walsh, R. *J. Chem. Soc., Chem. Commun.* **1985**, 964.
(41) Doering, W. von E.; Roth, W. R.; Breuckmann, R.; Figge, L.; Lennartz, H.-W.; Fessner, W.-D.; Prinzbach, H. *Chem. Ber.* **1988**, *121*, 1.
(42) Klumpp, G. W.; Stapersma, J. *J. Chem. Soc., Chem. Commun.* **1980**, 670.
(43) Stapersma, J.; Rood, I. D. C.; Klumpp, G. W. *Tetrahedron* **1982**, *38*, 2201.
(44) Meier, H.; Hanold, N.; Molz, T.; Bissinger, H. J.; Kolshorn, H.; Zountsas, J. *Tetrahedron* **1986**, *42*, 1711.
(45) Martin, H.-D.; Urbanek, T.; Walsh, R., to be published.
(46) Meier, H.; Pauli, A.; Kolshorn, H.; Kochhan, P. *Chem. Ber.* **1987**, *120*, 1607.
(47) Pauli, A.; Kolshorn, H.; Meier, H. *Chem. Ber.* **1987**, *120*, 1611.
(48) $\Delta H°(4 \rightarrow 23) = 34(\pm 6)$ kcal·mol^{-1}. Walsh, R., unpublished estimate.
(49) Hassenrück, K.; Martin, H.-D.; Mayer, B.; Urbanek, T.; Zirwes, T.; Walsh, R.; Beckhaus, H.-D. *Chem. Ber.* **1987**, *120*, 177.
(50) Smith, L. R.; Gream, G. E.; Meinwald, J. *J. Org. Chem.* **1977**, *42*, 927.
(51) Christl, M.; Lang, R. *J. Am. Chem. Soc.* **1982**, *104*, 4494.
(52) Meinwald, J.; Schmidt, D. *J. Am. Chem. Soc.* **1969**, *91*, 5877.
(53) Meinwald, J.; Tsuruta, H. *J. Am. Chem. Soc.* **1969**, *91*, 5877.
(54) Zimmerman, H. E.; Robbins, J. D.; Schantl, J. *J. Am. Chem. Soc.* **1969**, *91*, 5878.
(55) Iwamura, H.; Kihara, H. *Chem. Lett.* **1973**, 71.
(56) Baldwin, J. E.; Andrist, A. H. *J. Am. Chem. Soc.* **1971**, *93*, 3289.
(57) Frey, H. M.; Hopkins, R. G. *J. Chem. Soc. B* **1970**, 1410.
(58) Paquette, L. A.; Russell, R. K.; Wingard, R. E. *Tetrahedron Lett.* **1973**, 1713.
(59) Avram, M.; Dinulescu, I. G.; Marcia, E.; Mateescu, G.; Sliam, E.; Nenitzescu, C. D. *Chem. Ber.* **1964**, *97*, 382.
(60) Frey, H. M.; Martin, H.-D.; Hekman, M. *J. Chem. Soc., Chem. Commun.* **1975**, 204.
(61) Case, R. S.; Dewar, M. J. S.; Kirschner, S.; Pettit, R.; Slegir, W. *J. Am. Chem. Soc.* **1974**, *96*, 7581.
(62) Goldstein, M. J.; Leight, R. S. *J. Am. Chem. Soc.* **1977**, *99*, 8112.
(63) Martin. H.-D.; Hekman, M. *Angew. Chem., Int. Ed. Engl.* **1976**, *15*, 431.
(64) Zimmerman, H. E.; Grunewald, G. L. *J. Am. Chem. Soc.* **1966**, *88*, 183.
(65) Cheng, A. K.; Anet, F. A. L.; Mioduski, J.; Meinwald, J. *J. Am. Chem. Soc.* **1974**, *96*, 2887. (a) Moskau, D.; Aydin, R.; Leber, W.; Günther, H.; Quast, H.; Martin, H.-D.; Hassenrück, K.; Grohmann, K., to be published.
(66) Miller, R. D.; Yannoni, C. S. *J. Am. Chem. Soc.* **1980**, *102*, 7396.
(67) Macho, V.; Miller, R. D.; Yannoni, C. S. *J. Am. Chem. Soc.* **1983**, *105*, 3735.
(68) Hoffmann, R.; Stohrer, W.-D. *J. Am. Chem. Soc.* **1971**, *93*, 6941.
(69) Dewar, M. J. S.; Lo, H. D. *J. Am. Chem. Soc.* **1971**, *93*, 7201.
(70) Miller, L. S.; Grohmann, K.; Dannenberg, J. J. *J. Am. Chem. Soc.* **1983**, *105*, 6862.
(71) Dewar, M. J. S.; Jie, C. *Tetrahedron* **1988**, *44*, 1351.
(72) Dudek, D.; Glänzer, K.; Troe, J. *Ber. Bunsenges. Phys. Chem.* **1979**, 83, 776.
(73) Zimmerman, H. E.; Iwamura, H. *J. Am. Chem. Soc.* **1970**, *92*, 2015.
(74) Criegee, R.; Askani, R. *Angew. Chem., Int. Ed. Engl.* **1968**, *7*, 537.
(75) Huisgen, R.; Mietzsch, C. F. *Angew. Chem., Int. Ed. Engl.* **1964**, *3*, 83. (a) Vogel, E.; Kiefer, H.; Roth, W. R. *Angew. Chem.* **1964**, *76*, 432.
(76) Willstätter, R.; Waser, E. *Ber. Dtsch. Chem. Ges.* **1911**, *44*, 3423.
(77) Wipff, G.; Wahlgren, U.; Kochanski, E.; Lehn, J. M. *Chem. Phys. Lett.* **1971**, *11*, 350.
(78) Naor, R.; Luz, Z. *J. Chem. Phys.* **1982**, *76*, 5662.
(79) Paquette, L. A.; Oku, M.; Heyd, W. E.; Meisinger, R. H. *J. Am. Chem. Soc.* **1974**, *96*, 5815.
(80) Tanaka, J. *J. Chem. Soc. Jpn., Pure Chem. Sect.* **1954**, *75*, 212.
(81) Jones, M.; Schwab, L. O. *J. Am. Chem. Soc.* **1968**, *90*, 6549.
(82) Urbanek, T. Dissertation, Universität Düsseldorf, 1986.
(83) Flowers, M. C.; Frey, H. M. *J. Am. Chem. Soc.* **1972**, *94*, 8636.
(84) Brauman, J. I.; Farneth, W. E.; D'Amore, M. B. *J. Am. Chem. Soc.* **1973**, *95*, 5043; **1976**, *98*, 5546.
(85) Andrews, G. D.; Baldwin, T. E. *J. Am. Chem. Soc.* **1977**, *99*, 4853.
(86) Hassenrück, K.; Martin, H.-D.; Urbanek, T.; Walsh, R.; Watts, I. M., to be published.
(87) Robinson, P. J.; Holbrook, K. A. *Unimolecular Reactions*; Wiley: London, 1972; Chapters 8 and 10.
(88) Rossi, M. J.; Pladziewicz, J. R.; Barker, J. R. *J. Chem. Phys.* **1983**, *78*, 6695.
(89) Hippler, H.; Troe, T.; Wendelken, H. T. *J. Chem. Phys.* **1983**, *78*, 6709, 6718.
(90) Heymann, M.; Hippler, H.; Troe, T. *J. Chem. Phys.* **1984**, *80*, 1853.
(91) Dudek, D.; Glänzer, K.; Troe, J. *Ber. Bunsenges. Phys. Chem.* **1979**, *83*, 788.
(92) Zimmerman, H. E.; Binkley, R. W.; Givens, R. S.; Grunewald, G. L.; Sherwin, M. A. *J. Am. Chem. Soc.* **1969**, *91*, 3316.
(93) Zimmerman, H. E.; Boettcher, R. J.; Buehler, N. E.; Keck, G. E.; Steinmetz, M. G. *J. Am. Chem. Soc.* **1976**, *98*, 7680.
(94) Stapersma, J.; Klumpp, G. W. *Recueil, J. R. Neth. Chem. Soc.* **1982**, *101*, 274.
(95) Hixson, S. S.; Mariano, P. S.; Zimmerman, H. E. *Chem. Rev.* **1973**, *73*, 531. (a) Meinwald, J.; Tsuruta, H. *J. Am. Chem. Soc.* **1970**, *92*, 2579.
(96) Osawa, E.; Aigami, K.; Inamoto, Y. *J. Org. Chem.* **1977**, *42*, 2621 and references therein.
(97) Martin, H.-D.; Urbanek, T.; Walsh, R.; Hassenrück, K.; Mayer, B., unpublished results.
(98) Srinivasan, R.; Epling, G., unpublished results. Private communication from R. Srinivasan.
(99) Miridicyan, E.; Leach, S. *Bull. Soc. Chim. Belg.* **1962**, *71*, 845.
(100) Fonken, G. J. *Chem. Ind. (London)* **1963**, 1625.

(101) Turro, N. J.; Liu, J.-M.; Zimmerman, H. E.; Factor, R. E. *J. Org. Chem.* **1980**, *45*, 3511.
(102) White, E. H.; Friend, E. W.; Stern, R. L.; Maskill, H. *J. Am. Chem. Soc.* **1969**, *91*, 523.
(103) Yu, C. F.; Young, F.; Bersohn, R.; Turro, N. J. *J. Phys. Chem.* **1985**, *89*, 4409.
(104) Cassar, L.; Eaton, P. E.; Halpern, J. *J. Am. Chem. Soc.* **1970**, *92*, 3515.
(105) Cassar, L.; Eaton, P. E.; Halpern, J. *J. Am. Chem. Soc.* **1970**, *92*, 6366.
(106) Byrd, J. E.; Cassar, L.; Eaton, P. E.; Halpern, J. *J. Chem. Soc., Chem. Commun.* **1971**, 40.
(107) Merk, W.; Pettit, R. *J. Am. Chem. Soc.* **1967**, *89*, 4788.
(108) Hoffmann, R. *Acc. Chem. Res.* **1971**, *4*, 1.
(109) Hoffmann, R.; Heilbronner, E.; Gleiter, R. *J. Am. Chem. Soc.* **1970**, *92*, 706.
(110) Gassman, P. G.; Yamaguchi, R.; Koser, G. F. *J. Org. Chem.* **1978**, *43*, 4392.
(111) Gassman, P. G.; Yamaguchi, R. *J. Am. Chem. Soc.* **1979**, *101*, 1308.
(112) Gassman, P. G.; Yamaguchi, R. *Tetrahedron* **1982**, *38*, 1113.
(113) Bodor, N.; Dewar, M. J. S.; Worley, S. D. *J. Am. Chem. Soc.* **1970**, *92*, 19.
(114) Dewar, M. J. S.; Worley, S. D. *J. Chem. Phys.* **1969**, *50*, 654.
(115) Bischof, P.; Eaton, P. E.; Gleiter, R.; Heilbronner, E.; Jones, T. B.; Musso, H.; Schmelzer, A.; Stober, R. *Helv. Chim. Acta* **1978**, *61*, 547.
(116) Scamehorn, C. A.; Hermiller, S. M.; Pitzer, R. M. *J. Chem. Phys.* **1986**, *84*, 833.
(117) Schulman, J. M.; Fischer, C. R.; Solomon, P.; Venanzi, T. J. *J. Am. Chem. Soc.* **1978**, *100*, 2949.
(118) Franklin, J. L.; Carroll, S. R. *J. Am. Chem. Soc.* **1969**, *91*, 5940.
(119) Rücker, C.; Hassenrück, K.; Mayer, B.; Martin, H.-D., to be published.
(120) Gleiter, R. *Top. Curr. Chem.* **1979**, *86*, 197.
(121) Hassenrück, K.; Martin, H.-D.; Mayer, B. *Chem. Ber.* **1988**, *121*, 373.
(122) Lindholm, E.; Asbrink, L. *Molecular Orbitals and Their Energies, Studied by the Semiempirical HAM Method*; Springer-Verlag: Berlin, 1985.
(123) Jonkers, G.; Van der Meer, W. J.; de Lange, C. A.; Baerends, E. J.; Stapersma, J.; Klumpp, G. W. *J. Am. Chem. Soc.* **1984**, *106*, 587.
(124) Bischof, P.; Heilbronner, E.; Prinzbach, H.; Martin, H.-D. *Helv. Chim. Acta* **1971**, *54*, 1072.
(125) Gleiter, R.; Bischof, P.; Gubernator, K.; Christl, M.; Schwager, L.; Vogel, P. *J. Org. Chem.* **1985**, *50*, 5064.
(126) Gleiter, R.; Bischof, P.; Christl, M. *J. Org. Chem.* **1986**, *51*, 2895.
(127) Gleiter, R.; Kobayashi, T. *Helv. Chim. Acta* **1971**, *54*, 1081.
(128) Bischof, P.; Gleiter, R.; Haider, R. *Angew. Chem.* **1977**, *89*, 122; *J. Am. Chem. Soc.* **1978**, *100*, 1036.
(129) Kanda, K.; Koremoto, T.; Imamura, A. *Tetrahedron* **1986**, *42*, 4169.
(130) Gleiter, R.; Heilbronner, E.; Hekman, M.; Martin, H.-D. *Chem. Ber.* **1973**, *106*, 28.
(131) Iwamura, H.; Kihara, H.; Morio, K.; Kunii, T. L. *Bull. Chem. Soc. Jpn.* **1973**, *46*, 3248.
(132) Bodor, N.; Chen, B. H.; Worley, S. D. *J. Electron Spectrosc. Relat. Phenom.* **1974**, *4*, 65.
(133) Lehn, J. M.; Wipff, G., private communication. Wipff, G. These, Université Louis Pasteur de Strasbourg, 1974.
(134) Heilbronner, E.; Schmelzer, A. *Helv. Chim. Acta* **1975**, *58*, 936.
(135) Spanget-Larson, J.; Gleiter, R.; Paquette, L. A.; Carmody, M. J.; Degenhardt, C. R. *Theor. Chim. Acta* **1978**, *50*, 145.
(136) Chiang, H. J.; Worley, S. D. *J. Electron Spectrosc. Relat. Phenom.* **1980**, *21*, 121.
(137) Martin, H.-D.; Mayer, B. *Angew. Chem.* **1983**, *95*, 281; *Angew. Chem., Int. Ed. Engl.* **1983**, *22*, 283. (a) Palmer, M. H.; Guest, M. F. *J. Mol. Struct.* **1987**, *158*, 215.
(138) Askani, R.; Gleiter, R.; Heilbronner, E.; Hornung, V.; Musso, H. *Tetrahedron Lett.* **1971**, 4461.
(139) Spectrum of **10**: K. Hassenrück, B. Mayer, and H.-D. Martin. Hassenrück, K. Dissertation, Universität Düsseldorf, 1988.
(140) Haselbach, E.; Heilbronner, E.; Schröder, G. *Helv. Chim. Acta* **1971**, *54*, 153.
(141) Palmer, M. H. *J. Mol. Struct.* **1987**, *161*, 333.
(142) Gedanken, A.; de Meijere, A. *J. Chem. Phys.* **1988**, *88*, 4153.
(143) Eland, D. *Int. J. Mass Spectrom. Ion Phys.* **1969**, *2*, 471.
(144) Batich, C.; Bischof, P.; Heilbronner, E. *J. Electron Spectrosc. Relat. Phenom.* **1972/1973**, *1*, 333 and references therein.
(145) Palmer, M. H. *J. Mol. Struct.* **1988**, *178*, 79.
(146) Kobayashi, T. *Phys. Lett.* **1979**, *70A*, 292.
(147) Jordan, K. D.; Burrow, P. D. *Chem. Rev.* **1987**, *87*, 557.
(148) Frey, W. F.; Compton, R. N.; Naff, W. T.; Schweinler, H. C. *Int. J. Mass Spectrom. Ion Phys.* **1973**, *12*, 19.
(149) Van-Catledge, F. A.; McBride, C. E. *J. Am. Chem. Soc.* **1976**, *98*, 304.
(150) Van-Catledge, F. A. *J. Am. Chem. Soc.* **1971**, *93*, 4365.
(151) Zuccarello, F.; Buemi, G.; Raudino, A. *J. Comput. Chem.* **1980**, *1*, 341.
(152) Briat, B.; Schooley, D. A.; Records, R.; Bunnenberg, E.; Djerassi, C. *J. Am. Chem. Soc.* **1967**, *89*, 7062.
(153) Christl, M. *Chem. Ber.* **1975**, *108*, 2781. Christl, M.; Herzog, C. *Chem. Ber.* **1986**, *119*, 3067.
(154) Della, E. W.; McCoy, E. F.; Patney, H. K.; Jones, G. L.; Miller, F. A. *J. Am. Chem. Soc.* **1979**, *101*, 7441.
(155) Cole, T. W.; Perkins, J.; Putnam, S.; Pakes, P. W.; Strauss, H. L. *J. Phys. Chem.* **1981**, *85*, 2185.
(156) Cyvin, S. J.; Cyvin, B. N.; Brunvoll, J. *Z. Naturforsch.* **1983**, *38a*, 1248.
(157) Almlöf, J.; Jonvik, T. *Chem. Phys. Lett.* **1982**, *92*, 267.
(158) Dünn, K. M.; Pulay, P.; van Alsenoy, C.; Boggs, J. E. *J. Mol. Spectrosc.* **1984**, *103*, 268.
(159) Pine, A. S.; Maki, A. G.; Robiette, A. G.; Krohn, B. J.; Watson, J. K. G.; Urbanek, Th. *J. Am. Chem. Soc.* **1984**, *106*, 891.
(160) Tabacik, V.; Blaise, P. *J. Raman Spectrosc.* **1987**, *18*, 229.
(161) Van-Catledge, F. A.; McBride, C. E. *J. Phys. Chem.* **1976**, *80*, 2987.
(162) Traetteberg, M.; Hagen, G.; Cyvin, S. J. *Z. Naturforsch.* **1970**, *25b*, 134.
(163) Fleischer, E. B. *J. Am. Chem. Soc.* **1964**, *86*, 3889.
(164) Almenningen, A.; Jonvik, T.; Martin, H.-D.; Urbanek, Th. *J. Mol. Struct.* **1985**, *128*, 239.
(165) Kovacevic, K.; Maksik, Z. B. *J. Org. Chem.* **1974**, *39*, 539.
(166) Maksik, Z. B.; Kovacevic, K.; Mogus, A. *Theor. Chim. Acta* **1980**, *55*, 127.
(167) Schubert, W.; Yoshimine, M.; Pacansky, J. *J. Phys. Chem.* **1981**, *85*, 1340.
(168) Van Alsenoy, C.; Scarsdale, J. N.; Schäfer, L. *J. Comput. Chem.* **1982**, *3*, 53.
(169) Allinger, N. L.; Eaton, P. E. *Tetrahedron Lett.* **1983**, *24*, 3697.
(170) Wang, Y. C.; Bauer, S. H. *J. Am. Chem. Soc.* **1972**, *94*, 5651.
(171) Yamamoto, S.; Nakata, M.; Fukuyama, T.; Kuchitsu, K.; Hasselmann, D.; Ermer, O. *J. Phys. Chem.* **1982**, *86*, 529. Ermer, O. *Tetrahedron* **1974**, *30*, 3103.
(172) Traetteberg, M. *Acta Chem. Scand.* **1966**, *20*, 1724.
(173) Claus, K. H.; Krüger, C. *Acta Crystallogr.* **1988**, *C44*, 1632.